Check for updates

View Article Online
View Journal

Lab on a Chip

Devices and applications at the micro- and nanoscale

Accepted Manuscript

This article can be cited before page numbers have been issued, to do this please use: S. Kouthouridis, P. Saha, M. Ludlow, B. Y. Truong and B. Zhang, *Lab Chip*, 2025, DOI: 10.1039/D5LC00075K.

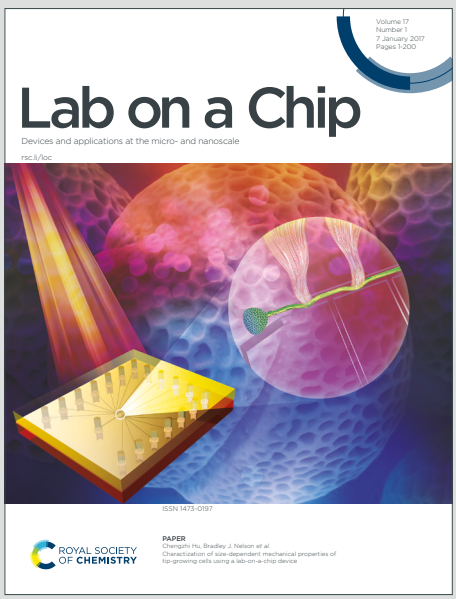

This is an Accepted Manuscript, which has been through the Royal Society of Chemistry peer review process and has been accepted for publication.

Accepted Manuscripts are published online shortly after acceptance, before technical editing, formatting and proof reading. Using this free service, authors can make their results available to the community, in citable form, before we publish the edited article. We will replace this Accepted Manuscript with the edited and formatted Advance Article as soon as it is available.

You can find more information about Accepted Manuscripts in the Information for Authors.

Please note that technical editing may introduce minor changes to the text and/or graphics, which may alter content. The journal's standard Terms & Conditions and the Ethical guidelines still apply. In no event shall the Royal Society of Chemistry be held responsible for any errors or omissions in this Accepted Manuscript or any consequences arising from the use of any information it contains.

View Article Online
DOI: 10.1039/D5LC00075K

Late-stage placental barrier model for transport studies of prescription drugs during pregnancy

Sonya Kouthouridis[1], Poonam Saha[2], Madeleine Ludlow[3], Brenda YN Truong[3], Boyang Zhang[1,3*].

[1] *Department of Chemical Engineering, McMaster University, Hamilton, ON, L8S 4L8, Canada*
[2] *Michael G. DeGroote School of Medicine, McMaster University, Hamilton, ON, L8S 4L8, Canada*
[3] *School of Biomedical Engineering, McMaster University, Hamilton, ON, L8S 4L8, Canada*

Open Access Article. Published on 27 May 2025. Downloaded on 6/4/2025 8:36:13 AM.
This article is licensed under a Creative Commons Attribution 3.0 Unported Licence.

Keywords

Placenta, barrier, drug permeability, high-throughput device, pregnancy, vasculature.

Abstract

Throughout pregnancy, the placental barrier is crucial for fetal development, evolving continuously to meet the growing nutritional demands of the fetus. Although the placenta has the capacity to selectively filter compounds, harmful xenobiotic substances from the maternal blood can sometimes cross over into the fetal circulation. This drives the development of *in vitro* placental barrier models in the context of drug transport studies. In this work, we adapted our lab's previous placental barrier model to transplacental drug transport by transitioning from self-assembled vasculature to a simplified straight tubular vasculature to improve throughput and consistency. We then closely examined the angiogenic cytokine secretion and crosstalk between trophoblasts and endothelial cells. Furthermore, we validated this model for drug barrier studies by assessing the permeability of three model therapeutic agents: paclitaxel, vancomycin, and IgG. Drug permeabilities were shown to be drug type, concentration, and size dependent, similar to what has previously been reported. The presented model offers a promising tool for enhancing drug safety assessments in pregnant women, ensuring both maternal well-being and fetal health.

Introduction

Throughout pregnancy, the placental barrier continuously evolves to accommodate the nutritional demands of the developing fetus. At term, the placenta consists of branched chorionic villi which are bathed in a chamber of maternal blood and house the fetal vascular (**Figure 1**). A thin layer of fused syncytiotrophoblasts (STs) enclose these villi and a smaller population of undifferentiated cytotrophoblast cells (CTs), and various stromal cells are present between this syncytium and the endothelial layer constructing the fetal vasculature. Along with nutrients, waste and gases, drugs entering the maternal blood stream can sometimes cross the placental barrier. Prescription drug use during pregnancy is often essential for maternal health and has steadily increased over the past three decades, particularly during the first trimester of gestation(1). These medications range from antibiotics—comprising 80% of all prescriptions during pregnancy(2)—to psychotropics and chemotherapeutics. The most commonly prescribed psychotropics for anxiety and depression are selective serotonin uptake inhibitors (SSRIs) and benzodiazepine (BZDs)(3) which have been shown to readily cross the placenta(4) and accumulate in fetal tissues(5,6). In the instance of maternal infection, antibiotics may be prescribed to pregnant women, despite being shown to cross the placental barrier(7) and cause increased risks of asthma and changes in

Lab on a Chip Accepted Manuscript

View Article Online
DOI: 10.1039/D5LC00075K

Open Access Article. Published on 27 May 2025. Downloaded on 6/4/2025 8:36:13 AM.
This article is licensed under a Creative Commons Attribution 3.0 Unported Licence.

the fetal intestinal microbiome(8). Alternatively, chemotherapy use during the first trimester is dangerous and can lead to the spontaneous termination of the pregnancy, therefore it is more likely to be prescribed during the 2nd and 3rd trimesters, when the risk of severe complications is reduced(9). However, many studies evaluating the safety and side effects of these drugs are contradictory, which make it difficult to conclusively judge their safety(10,11). Despite the potential negative side effects associated with these medications, it is crucial that pregnant women maintain access to them. The untreated ailments may pose greater risks than the listed side effects, therefore physicians must carefully weigh the necessity of treatment against the potential risks posed by the drugs. *In vitro* placental barrier models offer an ethical avenue to inform these decisions, facilitating the testing of drug treatment plans and the development of novel medications.

Many *in vitro* systems have been developed to mimic the placental barrier(12), however many of them have not successfully coupled a highly-differentiated ST layer with perfusable vasculature. In our previous work, we established a vascularized placental IFlowPlate model to model both early- and late-stage pregnancy which highlighted the importance of the vascular barrier in transplacental research(13). This model exhibited impressive ST fusion rates, averaging 84.4 ± 1.0%, and featured self-assembled vasculature, enabling the development of intricate vascular networks that closely mimic physiological conditions. However, while these networks offer enhanced realism and permit the study of drugs on vasculogenesis, they pose challenges to reproducibility because of the unguided self-assembly of the cells. Further, lung fibroblasts were used in these tissues as they are commonly used to support vascular self-assembly. In addition, this model required further validation to determine its effectiveness in drug transport studies.

To address some of these issues, we have streamlined our placental barrier model design by replacing the self-assembled vascular network with a single tubular blood vessel. This design change improved model consistency and experimental throughput as fewer cells are needed initially. In addition, without the need to optimize vascular self-assembly, there were greater freedom to use different types of vascular stromal cells. For our placenta models, placental pericytes were incorporated into the hydrogel matrix, in the place of conventional lung fibroblasts, to assess their capacity to support the vasculature of our model. Finally, this new model was used to assess the permeability of the commonly prescribed chemotherapeutic drug paclitaxel, the antibiotic vancomycin, and human immunoglobulin G (IgG) derived from human serum. The results demonstrated that placental permeability was dependent on both molecule size and concentration. Notably, fetal-to-maternal (F/M) concentration ratios were lowest for larger molecules, such as IgG and 65 kDa dextran, which crossed the placental barrier at significantly lower rates compared to smaller molecules like paclitaxel or vancomycin. Importantly, the model accurately reproduced the *ex vivo* permeability trends observed in placental explant perfusion studies for all three molecules.

Materials and Methods

Cell culture

Placenta stem cells (PSCs) (blastocyst-derived, RCB-4940, female) were procured from Riken BRC Cell Bank at passage number 17 and used until passage 23 in all experiments. Undifferentiated cells were maintained in expansion medium(14) consisting of DMEM/F12 + GlutaMAX supplemented with 2-mercaptoethanol (0.1×10^{-3} m), fetal bovine serum (FBS, 0.2%), penicillin–streptomycin (0.5%), bovine serum albumin (BSA, 0.3%), ITS (insulin, transferrin, selenium) media supplement (1%), L-ascorbic acid (1.5 µg mL^{-1}), EGF (50 ng mL^{-1}), CHIR99021 (2×10^{-6} m), A83-01 (0.5×10^{-6} m), SB431542 (1×10^{-6} m), VPA

Lab on a Chip Accepted Manuscript

View Article Online
DOI: 10.1039/D5LC00075K

Open Access Article. Published on 27 May 2025. Downloaded on 6/4/2025 8:36:13 AM.
This article is licensed under a Creative Commons Attribution 3.0 Unported Licence.

(0.8×10^{-3} m), and Y27632 (5×10^{-6} m). T75 flasks were precoated with a 10 µg/ml col IV solution in PBS and incubated for 1.5 hours at 37°C. Cells were passaged when they reached 80% confluence by washing with PBS, then dissociating with TrypLE for 10-15 mins and splitting at a 1:4 ratio onto collagen IV-coated flasks. Primary human umbilical vascular endothelial cells (HUVECs) were purchased from CedarLane Labs (CAP-0001GFP) and expanded in endothelial cell growth medium 2 (ECGM2, Sigma-Aldrich, C22011) supplemented with 1% antibiotic/antimycotic (100x, Sigma-Aldrich, A5955-100ML), on flasks coated with 0.2% gelatin, until passage 5. HUVEC/TERT2 cells were obtained from Evercyte (CHT-006-0008) and were expanded in ECGM2 supplemented with G418 (InvivoGen, ant-gn-1), an antibiotic acting as a selection agent to maintain the purity of the transfected culture. Both HUVEC types were dissociated with Trypsin-EDTA solution (0.05%) for 3 minutes at 37°C and replated at a 1:4 ratio. Primary human placental pericytes (hPC-PL) were obtained from PromoCell (C-12980), cultured in pericyte growth medium 2 (PGM2, Millipore Sigma, C-28041) and used until passage 5. Pericytes were dissociated with StemPro™ Accutase™ (Thermofisher, A1110501) for 2-4 mins at room temperature and replated at a 1:4 ratio according to the cell bank's instructions. All cells were cultured at 37°C with 5% CO_2.

AngioPlate manufacturing

The AngioPlate manufacturing protocol used in this work was adapted from the methods developed by Zhang et al(15). Briefly, a 40% gelatin solution was prepared by dissolving gelatin from bovine skin (Sigma Aldrich, G9391) in water and autoclaving to dissolve and sterilize. Gelatin fibers were 3D printed onto pressure-adhesive sheets on a BIO X™ (Cellink) bioprinter with a 30G needle. The resulting gelatin channels had a diameter of 200 µm and were printed in a 384-well plate format. The patterned sheet was subsequently capped onto the base of a bottomless 384-well plate which had been milled with channels to accommodate the gelatin structures. Plates were UV sterilized for 10 minutes each side before use. These plates are also commercially available from OrganoBiotech (A002).

Establishment of model

A prepolymer fibrin gel solution was prepared by mixing 125 µL of 10mg/ml fibrinogen (Sigma-Aldrich, F3879) with 25 µL of 10U/ml thrombin (Sigma-Aldrich, T6884) in a 1.5ml Eppendorf tube. 25 µL gels were immediately cast into the center wells of each AngioPlate device and allowed to crosslink at room temperature for 30 mins. 90 µL of warmed PBS was added to each well and the plate was placed on a rocker (OrganoBiotech, B001) at 30°C for 20 mins to wash away the sacrificial gelatin channels. PBS was replaced and plate was incubated in the same conditions for another 20 minutes. PBS was then aspirated and 50 µL of ECGM2 supplemented with 1% aprotinin was added to each center well and 90 µL into each adjacent well before placing the plate on the 37°C rocker overnight. The next day, media was aspirated from all wells, being careful not to disturb the fibrin gel in the center compartments. A cell suspension of 500,000 HUVECs/ml was prepared and 120 µL was pipetted into both compartments adjacent to the gel. The hydrostatic pressure difference between the center and adjacent wells allows the cells to flow into the fibrin channel, which eventually becomes the vascular channel. Once seeded, the plate is incubated flat for 2 hours at 37°C before 50 µL of media was added to the central gel. Media was changed daily by pipetting 50 µL into the center well and 80 µL into each adjacent well. On day 7 of culture, PSCs were added to the central compartment to form a monolayer of STs. Firstly, a 400,000 cell/ml suspension of PSCs was prepared in ST media(13,14) consisting of DMEM/F12 + GlutaMAX supplemented with 100 mM 2-mercaptoethanol, 0.5% penicillin–streptomycin, 0.3% BSA, 1% ITS media supplement, 25 µM Y27632, 2 µM forskolin, 4% KSR and 1% aprotinin. 60 µL of cell suspension were added to the central compartment and media was switched to a compartmentalized setup for the rest of the culture with ST media in the

Lab on a Chip Accepted Manuscript

View Article Online
DOI: 10.1039/D5LC00075K

center and ECGM2 in the adjacent wells. Media was changed daily, and barrier analyses were performed after 8 days of coculture to allow for ST differentiation.

Incorporation of pericytes in model

Placental pericytes were incorporated into some models to determine where they improve vascular barrier and/or placental barrier permeability. Before casting, the prepolymer fibrin gel solution was laden with pericytes at concentrations of either 50,000 cells/ml or 25,000 cells/ml. Gels were washed twice with PBS for 20 minutes, similar to the standard AngioPlate protocol above, however, 8% FBS was added to the ECGM2 media overnight to promote pericyte growth. Media was changed daily and HUVECs were added on day 2 of culture after which media was switched to ECGM2 without FBS. PSCs were added 7 days later, and cultures were maintained as described in the previous section. All media added to the platform included 1% aprotinin to control fibrin degradation over time.

Vascular permeability assay

A vascular permeability assay was performed before commencing coculture to confirm that the vasculature had formed correctly, and, once again, before every total barrier permeability assay to verify that vascular integrity was maintained during coculture. A solution of 1 mg/ml of TRITC-labelled 65 kDa dextran (Sigma-Aldrich, T1162) and 1 mg/ml of FITC-labelled 4 kDa dextran (Sigma-Aldrich, 46944) was prepared in media. A standard curve was prepared by serially diluting the dextran solution (1:1, 1:10, 1:100, 1:1000 and 0 mg/ml) and pipetting 90 µL into each of three standard replicates. All media aspirated from the plate, and 65 µL of fresh media was added to the center gel. Next, 90 µL of dextran solution was added to both adjacent wells to normalize the hydrostatic head in all three interconnect wells (90 µL dextran, 65 µL media + 25 µL gel, 90 µL dextran). Fluorescent measurements were immediately acquired with a Cytation5 plate reader and acquired again after placing the plate on the rocker for 1 hr to determine vascular permeability under realistic culture conditions. When performing this assay in coculture, dextran solutions, as well as standard curves were prepared in 50/50 mixtures of the media used in the compartmentalized cultures. All data presented in the same plots were performed on the same day.

Total permeability assay

Total dextran permeability of the AngioPlate placental barrier model by measuring the amount of dextran that diffused from the maternal compartment (central well above the STs) through the ST and endothelial layers, into the fetal compartments (adjacent wells). 4 kDa and 65 kDa fluorescently labeled dextrans were added into the maternal compartment at a 1:1 molar ration (12.34 µg/ml and 200 µg/ml, respectively) in mixed media consisting of isovolumetric amounts of ECGM2 and STM. At t=0 of this assay, media was aspirated from all wells and 100 µL of 1:1 ECGM2 and STM was added to the fetal wells. 75 µL of the dextran solution was added to the central maternal compartment of the device to equilibrate media levels between compartments and avoid flow (25 µL gel + 75 µL dextran = 100 µL in center well). The plate was placed on a rocker at 37°C for 24 hours, at which point fluorescent was analyzed to determine the amount of dextran permeated through the barrier model. Standard curves were prepared in a 1:1 media ratio of ECGM2:STM to determine the final dextran concentrations in the fetal compartments. Fluorescent measurements were acquired using the Cytation7 plate reader. The absence of bleed-through between channels was confirmed in previous work(13).

Open Access Article. Published on 27 May 2025. Downloaded on 6/4/2025 8:36:13 AM.
This article is licensed under a Creative Commons Attribution 3.0 Unported Licence.

Lab on a Chip Accepted Manuscript

View Article Online
DOI: 10.1039/D5LC00075K

Open Access Article. Published on 27 May 2025. Downloaded on 6/4/2025 8:36:13 AM.
This article is licensed under a Creative Commons Attribution 3.0 Unported Licence.

Immunostaining

AngioPlate gels were first washed with PBS for 5 mins and then fixed with a 4% paraformaldehyde solution overnight in a 4°C fridge, where all overnight immunostaining steps were performed. The next day, gels were washed with PBS three times for 10 mins each and then fresh PBS was added overnight to remove any residual fixative. Cells were blocked and permeabilized overnight with a 10% FBS (Thermo Fisher Scientific, 12484028) and 0.1% triton-X (Sigma-Aldrich, X100) in PBS solution. Next, a primary antibody solution was prepared consisting of either anti-e-cadherin (1:200 dilution, Invitrogen, 13-1700), anti-ve-cadherin (1:1000, abcam, ab33168), anti-MRP1/P-gp (1:250, Enzo Life Sciences, ALX-801-007), anti-MDR1 (1:50, Santa Cruz Biotechnologies, sc-55510) or anti-hCG (1:100, Sigma-Aldrich, SAB4500168)diluted in 2% FBS. Samples were incubated in the primary antibody solution overnight and washed thrice with PBS for 10 mins. A secondary antibody solution consisting of anti-mouse FITC (1:1000 dilution, Sigma-Aldrich, F0257) or anti-rabbit CF594 (1:200, Sigma-Aldrich, SAB4600107-250UL), anti-rat Alexa 488 (1:500, Thermofisher, A11006) or anti-mouse CF 594 (1:200, Sigma-Aldrich, SAB4600105) and DAPI (1:1000, Sigma-Aldrich, D9542) in 2% FBS was applied to the gels overnight. The next day, tissues were washed in PBS thrice for 10 mins, before being washed with fresh PBS overnight again. Samples were manually removed from the plate and imaged in a chamber slide via confocal microscopy (3i Marianas Lightsheet microscope).

Fusion percent quantification

Fusion analysis was performed on confocal images of tissues stained for DAPI and e-cadherin. Total cell number was determined by counting DAPI-stained nuclei in imageJ. The e-cadherin stain was superimposed onto the DAPI image, and the fusion percent was determined by counting nuclei present in groups of at least three within a single e-cadherin boundary. The fusion percent was reported as the ratio between the number of fused nuclei and the number of total nuclei in each image.

Drug permeability assay

The drug permeability assay was designed in a similar way to the dextran permeability assay, where fluorescent-labeled versions of the drugs were introduced into the central maternal compartment of the placental model and incubated for 24 hrs, then fluorescent readings of the adjacent fetal compartments were taken to determine drug concentrations. Paclitaxel (Oregon Green Conjugate, Sigma Aldrich, P22310) solutions were prepared at concentrations of 5 μM, 500 nM, and 50 nM in the 1:1 ECGM2: STM mixed media. Vancomycin (FITC Conjugate, Sigma Aldrich, SBR00028) solutions were also prepared at concentrations of 5 μg/ml, 500 ng/ml, and 50 ng/ml in the 1:1 ECGM2: STM mixed media. Finally, an IgG solution (FITC conjugate, Sigma Aldrich, F9636) of 1 mg/ml was prepared in the same media. At t=0 of this assay, media was aspirated from all wells and 100 μL of 1:1 ECGM2 and STM was added to the fetal wells (left and right). 75 μL of one of the drug solutions were added to the central maternal compartment of the device. The plate was placed on a rocker at 37°C for 24 hours and 70 μL of media was sampled from the fetal wells and pipetted into a black-walled and clear bottomed 384-well plate for fluorescent analysis. Standard curves for each one of these drugs were prepared in a 1:1 media ratio of ECGM2:STM to determine the final drug concentrations in the fetal compartments. Fluorescent measurements were acquired using the Cytation7 plate reader at the excitation/emission wavelengths specified by the drugs' manufacturer.

Lab on a Chip Accepted Manuscript

View Article Online
DOI: 10.1039/D5LC00075K

Open Access Article. Published on 27 May 2025. Downloaded on 6/4/2025 8:36:13 AM.
This article is licensed under a Creative Commons Attribution 3.0 Unported Licence.

Angiogenic cytokine analysis

AngioPlate tissues were cultured for 15 days with daily media changes to allow for ST differentiation. 24 hours after the last media change, supernatant from the central (apical) compartment and media from the adjacent (basolateral) compartments were collected. Media supernatant was centrifuged at 1000g for 10 minutes to precipitate any cell debris, and 70 μL of each sample was collected from the top surface of the vial. Samples were stored in -80°C until they were sent to Eve Technologies for cytokine analysis. Samples were analyzed using the Human Angiogenesis & Growth Factor 17-Plex Discovery Assay® (HDAGP17) for the following biomarkers: Angiopoietin-2, BMP-9, EGF, Endoglin, Endothelin-1, FGF-1, FGF-2, Follistatin, G-CSF, HB-EGF, HGF, IL-8, Leptin, PLGF, VEGF-A, VEGF-C, VEGF-D. Secretion values under the detectable limit of the assay were presenting as OOR (out of range).

Statistical analysis

All plots and statistics were performed using either paired t-test or one-way ANOVAs with Sidak multiple comparison in the GraphPad Prism software with 95% confidence ($\alpha = 0.05$, $p < 0.05$). Normality was tested using Shapiro–Wilk test and equal variance was tested using F-test. Data in all graphs were plotted as means with standard deviation as error bars.

Results

Model design

The late-stage placental barrier is primarily composed of a thin ST layer jacketing the chorionic villi, and an underlying endothelial layer that encloses the fetal blood (**Figure 1**). A defining feature of this stage is the presence of a fully developed, perfusable, and permeability-selective vascular network representing the fetal circulation. In our model, we have incorporated both the mature ST layer and this functional vascular component to more accurately recapitulate the structure and function of the late-stage placental barrier. When designing this placental barrier model for drug safety studies, we applied a similar approach to our previous model(13) where a ST barrier, a fibrin gel matrix and a vascular barrier separate the fetal and maternal compartments of the model (**Figure 1**). The stem cells used to form the ST layer of our placental barrier were derived using the protocol established by Okae et al.(14). In this study, we refer to these cells as placental stem cells (PSCs) to reflect their specific use in building placental tissue; however, they are functionally equivalent to the trophoblast stem cells (TSCs) described in the original Okae study. Further, the plate design is inspired from standard 384-well plates, enabling device compatibility with traditional imaging infrastructure and liquid handling tools. Wells are also connected in triplets (**Figure 1**) to allow for perfusion of media throughout the vascular channel when incubating the plate on a tilting device.

To accommodate the requirements of high-throughput drug safety studies, we transitioned from the self-assembled vascular networks in the IFlowPlate platform to a straight, uniform vascular channel in our placental AngioPlate device (**Figure 1**). The barrier's surface area plays a significant role in dictating both the rate and quantity of molecule permeation across a cell layer. Thus, ensuring consistency in barrier surface area across tissues is crucial for reliable comparisons of drug permeability data. This transition from self-assembled to straight vasculature not only increased tissue consistency but also eliminated the need for extensive optimization of culture conditions, resulting in a higher yield of perfusable tissues. Additionally, it improved model experimental throughput by reducing the initial cell requirements and offering greater flexibility in using various vascular stromal cell types. For instance, in some of our placenta

Lab on a Chip Accepted Manuscript

View Article Online
DOI: 10.1039/D5LC00075K

models, placental pericytes were incorporated into the hydrogel matrix as a replacement for lung fibroblasts from previous work to assess their capacity to support vascularization.

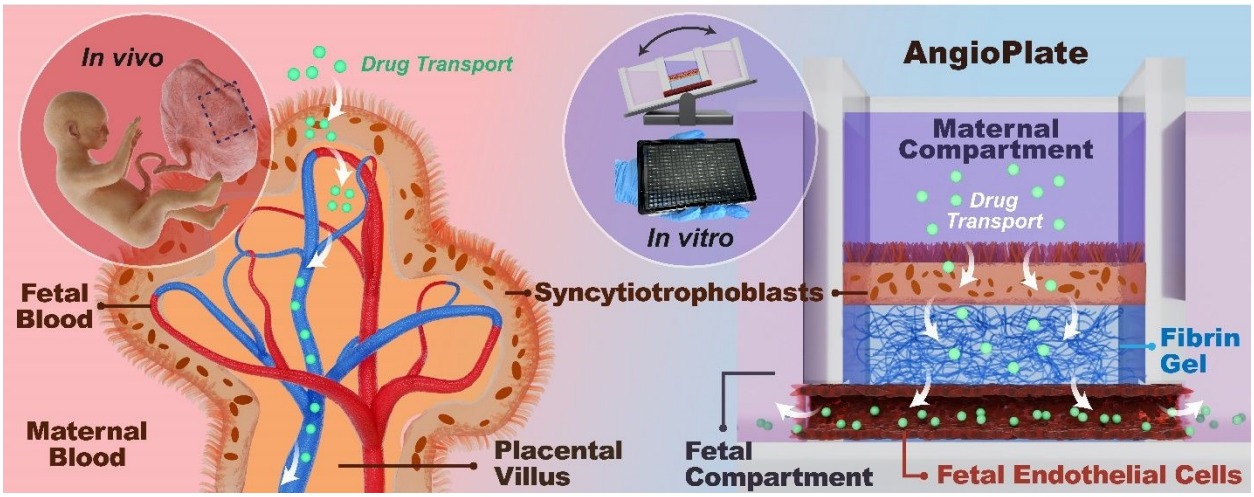

Figure 1. *Design of a single channel placental barrier model.* ***Left.*** *Placental chorionic villi consist of a thin multinucleated ST layer enclosing the fetal vasculature. Nutrients are transported from the maternal blood, through both the syncytial and endothelial barriers, to the fetal vasculature to meet the nutritional demands of the growing fetus.* ***Right.*** *The AngioPlate placental barrier model consists of a fibrin hydrogel acting as the interstitial space with a single vascular channel connecting it to the two adjacent wells. On the apical side of the gel, a ST monolayer is differentiated, and endothelial cells are seeded on the periphery of the vascular channel to form a vessel. The device is incubated on a tilting device which permits media perfusion to the vessel. The single channel placental barrier model is designed based on a 384-well plate and can accommodate high-throughput studies.*

To establish the model, we started with an AngioPlate with a sacrificial fiber patterned at the bottom of the well plate. Then a fibrin hydrogel was cast and crosslinked in the center well of the unit and the sacrificial template was dissolved away, resulting in a channel embedded in the hydrogel at the base of the central well. A ST layer was cultured on the surface of the gel, separating the gel from the central maternal compartment, whereas the fetal compartment consisted of the adjacent wells, connected by the endothelial-lined vascular channel (**Figure 1**). Vascular stromal cells can be embedded inside the fibrin gel surrounding the vascular channel as needed.

The effects of endothelial coculture on vascular barrier permeability

Establishing coculture models, especially with stem cells, can be challenging due to the unpredictable effects the media supplements of one cell type can have on the other. Further, cells release cytokines and other soluble factors that may affect the coculture's capacity to grow harmoniously. It is therefore imperative that coculture effects, as well as media effects are evaluated in this placental barrier model. To do this, we assessed the permeability of AngioPlate cultures consisting of human umbilical vascular endothelial cells (HUVECs in ECGM2 media) cocultured with placenta stem cells (PSCs) either in their undifferentiated CT-like state or after being differentiated into STs or extravillous cytotrophoblasts (EVTs) (**Figure 2A**). Fluorescently labeled 4 kDa and 65 kDa dextrans were perfused through the vascular channel for one hour on day 15 of culture and fluorescent readings were taken (**Figure 2BDE**). As anticipated, these cocultures resulted in confluent placental monolayers by day 15 with high fusion rates of 98.2 ± 0.2% and hCG secretion (**Figure 2C**). The hCG expression observed in the ST monolayer is consistent with previous results from our IFlowPlate model(13), which employed the same cell types under comparable experimental conditions, and who's extent of differentiation was validated via histology, fusion assay and gene expression analysis. To further confirm the specificity of hCG expression to differentiated STs, we

Open Access Article. Published on 27 May 2025. Downloaded on 6/4/2025 8:36:13 AM.
This article is licensed under a Creative Commons Attribution 3.0 Unported Licence.

Lab on a Chip Accepted Manuscript

View Article Online
DOI: 10.1039/D5LC00075K

Open Access Article. Published on 27 May 2025. Downloaded on 6/4/2025 8:36:13 AM.
This article is licensed under a Creative Commons Attribution 3.0 Unported Licence.

performed immunostaining in a non-differentiated control group and observed significantly lower hCG signal intensity, supporting the differentiation-dependent nature of hCG expression in our model (Supplementary **Figure S3**). This outcome aligns with their intrinsic epithelial characteristics, reflecting their functional roles at distinct stages of gestation within the placental barrier. When comparing coculture to the HUVEC only condition, the diffusion of both 4 kDa and 65 kDa dextrans was highest in the PSCs + HUVECs conditions (1013.0 ± 120.9 pmol/hr and 31.0 ± 4.6 pmol/hr, respectively), suggesting that either PSC expansion media was incompatible with HUVEC culture or that undifferentiated PSCs release factors that break down the endothelial barrier (**Figure 2BDE**). This could be due to the high media concentrations of valproic acid, a known HDAC inhibitor(16). It has been shown that HDAC inhibition can lead to endothelial disfunction(17,18), whereas HDAC activation has been shown to drive CT fusion(19). *In vivo*, undifferentiated CTs are most numerous and proliferative in the early stages of pregnancy, indicating HDAC inactivation, whereas vascular formation and syncytial fusion occur concurrently between the 4th and 10th weeks of gestation, indicating HDAC activation.

Surprisingly, HUVECs exhibited the second-weakest barrier permeability (901.4 ± 91.8 pmol 4 kDa dextran/hr and 26.4 ± 5.1 pmol 65 kDa dextran/hr) despite being cultured alone in their specialized medium (ECGM2), which has been proven to maintain their morphology up until the 10th passage(20). We hypothesize that this is due to the absence of stromal cells, which have been shown to support vascular formation and long-term stability in tissue engineered models(21–24). ST + HUVEC cocultures seemed to have improved barrier permeability of both 4 kDa (289.8 ± 128.0 pmol/hr) and 65 kDa dextran (6.3 ± 4.6 pmol/hr) when compared to the HUVEC only control, with the ST + HUVEC condition being the least permeable. The HUVEC + EVT condition had statistically similar permeabilities (406.5 ± 195.6 pmol/hr for 4 kDa dextran and 5.7 ± 4.8 pmol/hr for 65 kDa dextran). Once again, these permeability results parallel the PIBF1 secretion profiles presented by Lee *et al.* which showed that PSCs secreted the least amount of PIBF1 when compared to STs and EVTs(25). This is reasonable given that, in early-stage pregnancy, when CTs are present in large quantities, blood vessels have not yet been formed. However, in the second and third trimesters when STs make up a larger proportion of trophoblasts within the placenta, perfusable fetal vasculature has been established. These results suggest that ST culture media may be supporting and strengthening the vascular barrier, or these cell types may be secreting factors that benefit the long-term culture of endothelial cells. A similar experiment was performed using immortalized TERT-HUVECs and similar trends were observed (**Figure S2**).

The effects of endothelial coculture on angiogenic cytokine secretions

To explain the differences in vascular barrier integrity between HUVEC only and HUVEC + STs conditions, cell culture supernatant was sampled from each culture and analyzed for the secretion of angiogenic cytokines: angiopoietin-2, BMP-9, EGF, endoglin, endothelin-1, FGF-1, FGF-2, follistatin, G-CSF, HB-EGF, HGF, IL-8, leptin, PLGF, VEGF-A, VEGF-C and VEGF-D (**Figure 2H-N**, **Figure S1**). Although supernatant concentrations of angiopoietin-2, EGF, FGF-1, follistatin, G-CSF, HB-EGF, HGF, IL-8, VEG-C and VEG-D were statistically similar between these two culture conditions (**Figure 2FG**), we observed notable differences in 7 different cytokine profiles.

BMP-9 (bone morphogenetic protein 9) is a multifunctional protein and a member of the TGF-β family, whose main function consists of promoting bone and cartilage formation(26). BMP-9 supernatant concentrations increased from 0.2 ± 0.03 to 0.3 ± 0.04 pg/ml, a 1.4-fold change (**Figure 2F-H**), with the addition of STs to the culture. While trophoblasts contribute to placental development and vascularization, BMP-9 secretion by trophoblasts is not as well-documented or as prominent as its secretion by endothelial cells. STs may promote the production of BMP-9 in HUVECs to enhance

Lab on a Chip Accepted Manuscript

View Article Online
DOI: 10.1039/D5LC00075K

Open Access Article. Published on 27 May 2025. Downloaded on 6/4/2025 8:36:13 AM.
This article is licensed under a Creative Commons Attribution 3.0 Unported Licence.

angiogenesis and blood vessel formation, which is essential in pregnancy to support the growing fetus. Regardless, it has been shown that BMP-9 induces endothelial proliferation(27), which suggests that it may play a role in increasing the confluence of the vascular culture, as seen from the vascular permeability assays (**Figure 2DE**). A smaller 1.1-fold increase was observed for FGF-2, whose concentrations went from 1.4 ± 0.1 to 1.5 ± 0.1 ng/ml with the addition of the trophoblast cells, suggesting that STs might also be stimulating FGF-2 secretion in endothelial cells (**Figure 2FGK**). FGF-2 is a fibroblast growth factor known for its potent ability to stimulate the proliferation and differentiation of various cell types(28), as well as its role in tissue repair and regeneration(29). However, FGF-2 has also been shown to have angiogenic properties(30). Cao *et al.* showed that, when micropellets containing FGF-2 were implanted into the corneas of mice, they induced a high density of blood vessels with very few fenestrations and low permeability, demonstrated via a ferritin permeability assay(30). Therefore, similar to BMP-9, increased levels of FGF-2 in the media may be better maintaining the integrity of the vascular channel over long culture times.

Most drastically, leptin concentrations increased 171.2-fold when transitioning from the HUVEC monoculture to the HUVEC and ST coculture (**Figure 2FGL**). Outside of pregnancy, this hormone's main function in the human body is to regulate hunger and metabolic rates(31), however, during pregnancy, it plays a role in fetal development, nutrient transport, and angiogenesis(32). This steep increase in supernatant concentrations of leptin is unsurprising, given that it has been well-documented that placental trophoblasts secrete leptin(33) to modulate of embryo implantation, placental proliferation, as well as to further signal the metabolic demands and growth requirements of the developing fetus. However, leptin has been shown to activate angiogenesis(34) and to exert a protective effect on endothelial function(35), which may explain why vascular integrity was maintained longer when HUVECs were cocultured with STs (**Figure 2BDE**). The cytokine with the second highest fold increase is placental growth factor (PLGF), a member of the vascular endothelial growth factor (VEGF) family of proteins, with concentrations of 166.1 ± 44.1 pg/ml for the HUVEC only condition and 354.2 ± 21.9 pg/ml for HUVEC and ST coculture (2.1-fold increase, **Figure 2FGM**). PLGF is closely associated with placental development and has been known to enhance non-branching angiogenesis(36). In fact, it has been reported that PLGF is primarily secreted by both EVTs and villous cytotrophoblasts(36,37), however, it is also secreted by endothelial and endothelial cells(37). Although present in smaller concentrations, we see a similar trend in VEGF-A profiles when introducing STs to the HUVEC culture (2.2 ± 0.9 to 3.4 ± 1.0 pg/ml, 1.7-fold change, **Figure 2FGN**), which can be explained by the fact that VEGF-A and PLGF are part of the same family of VEGFs, both being key drivers in angiogenesis.

Interestingly, levels of both endoglin and endothelin-1 were higher in the HUVEC only condition (162.8 ± 21.2 and 92.0 ± 10.7 pg/ml, respectively), when compared to the corresponding coculture condition (125.4 ± 22.7 and 59.6 ± 11.8 pg/ml, respectively, **Figure 2FGIJ**). Endoglin is a co-receptor for TGF-β and is involved in angiogenesis and endothelial cell function. Lower levels of endoglin in the co-culture might reflect a feedback mechanism where STs downregulate endoglin to modulate the angiogenic response, possibly to prevent excessive or inappropriate vascular growth. Endothelin-1 is a potent vasoconstrictor that also has roles in inflammation and vascular remodeling. The reduced endothelin-1 in the co-culture could suggest that STs suppress its production to maintain a more relaxed vascular environment, which would be beneficial for ensuring adequate blood flow to the developing placenta.

The increased levels of angiogenic factors (BMP-9, FGF-2, leptin, PLGF, and VEGF-A) support the formation of new blood vessels, which is essential in pregnancy. In contrast, the decreased levels of endoglin and endothelin-1 may reflect a controlled environment to prevent excessive vasoconstriction

Lab on a Chip Accepted Manuscript

View Article Online
DOI: 10.1039/D5LC00075K

and to fine-tune the angiogenic process, ensuring a balanced and functional placental vasculature. Differences in the angiogenic cytokine profiles of these cultures suggest significant interactions between these two cell types that influence their behavior and the secretion of specific signaling molecules. The STs appear to influence HUVECs by modulating the secretion of cytokines and growth factors that are critical for angiogenesis and placental development.

Open Access Article. Published on 27 May 2025. Downloaded on 6/4/2025 8:36:13 AM.
This article is licensed under a Creative Commons Attribution 3.0 Unported Licence.

Lab on a Chip Accepted Manuscript

View Article Online
DOI: 10.1039/D5LC00075K

Open Access Article. Published on 27 May 2025. Downloaded on 6/4/2025 8:36:13 AM.
This article is licensed under a Creative Commons Attribution 3.0 Unported Licence.

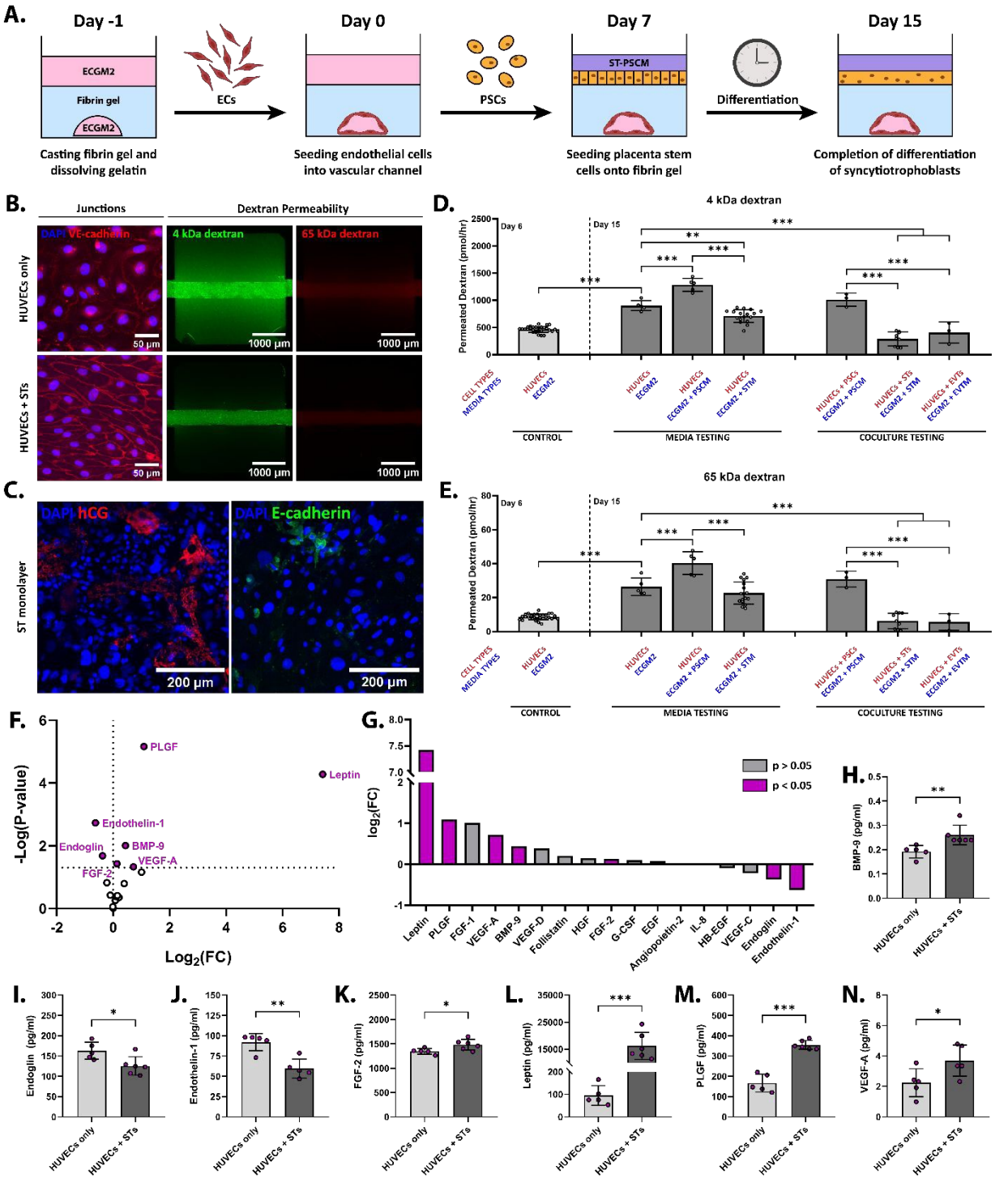

Figure 2. *The effects of ST coculture on endothelial barrier integrity and cytokine secretion.* ***A.*** *Timeline for placental barrier model establishment. On day -1, the fibrin hydrogel is cast, and the gelatin is allowed to dissolve with multiple PBS washes. On day 0, endothelial cells are seeded into the vascular channel and allowed to reach confluence before PSCs are added on day 7 and media is switched to compartmentalized culture. PSCs are differentiated into STs until day 15 when a dextran permeability analysis is usually performed.* ***B.*** *Immunostaining of endothelial junction marker VE-cadherin (red) and nucleic acids (DAPI, blue) in vascular tissues when cultured with and without differentiated STs. Fluorescent images of 4kDa (green) and 65 kDa (red) dextran permeation through endothelial channel after 1 hour of perfusion.* ***C.*** *hCG (red) and e-cadherin (green) immunostaining of ST monolayer in HUVECs + ST coculture condition.* ***D.*** *Vascular permeability values on days 6 and 15 for FITC-labelled 4 kDa dextran*

Lab on a Chip Accepted Manuscript

View Article Online
DOI: 10.1039/D5LC00075K

*after 1 hour of hydrostatic pressure-based vascular perfusion (two-way ANOVA, *p<0.05, **p<0.01, ***p<0.001). Media types and coculture conditions were tested. Datapoints from 3 separate experiments were combined in this plot.* ***E.*** *Vascular permeability values on days 6 and 15 for TRITC-labeled 65 kDa dextran after 1 hour of hydrostatic pressure-based vascular perfusion (N=3, two-way ANOVA, *p<0.05, **p<0.01, ***p<0.001). Media types and coculture conditions were tested. Datapoints from 3 separate experiments were combined in this plot.* ***F.*** *P-value as a function of fold change in angiogenic cytokine secretion. Fold change is calculated as the secretion in the HUVECs + STs condition divided by that of the HUVECs only condition.* ***G.*** *Fold change in angiogenic cytokine secretion when adding STs to vascular culture. Cytokines are ordered from highest to lowest fold change. Bars colored in magenta exhibit significant differences in angiogenic cytokine secretion between HUVECs only and HUVECs + STs conditions.* ***H-N.*** *Angiogenic cytokine secretion of HUVECs only and HUVECs + ST barrier models 24 hrs after media change. (N=5-6, t-tailed t-test, *p<0.05, **p<0.01, ***p<0.001).*

Open Access Article. Published on 27 May 2025. Downloaded on 6/4/2025 8:36:13 AM.
This article is licensed under a Creative Commons Attribution 3.0 Unported Licence.

The effects of media types on vascular barrier permeability

To decouple the effects of coculture and media type on vascular permeability, we next evaluated the permeability of the vascular channel cultured under different media conditions: ECGM2 only, compartmentalized media with PSCM in the center and ECGM2 in the adjacent compartments (ECGM2 + PSCM), and compartmentalized media with STM in the center and ECGM2 in the adjacent compartments (ECGM2 + STM). All three conditions were maintained exclusively in ECGM2 until day 6, mimicking the setup for coculture. On day 7, the mixed conditions were transitioned to compartmentalized media. As a result, the HUVECs cultured in ECGM2 on day 6 serve as the pre-compartmentalization control for all conditions. Dextran vascular permeability assays were performed both on day 6 and day 15 (**Figure 2DE**). Day 6 permeabilities to 4 kDa dextran ranged from 352.8 pmol/hr to 567.4 pmol/hr across all vascular tissues, and permeabilities to 65 kDa dextran ranged from 4.5 pmol/hr to 12.6 pmol/hr (**Figure 2DE**). Notably, vascular permeability in the HUVEC-only condition increased significantly from day 6 to day 15, indicating progressive barrier degradation over time. This functional decline is consistent with previous reports that VE-cadherin expression and endothelial integrity decrease in long-term HUVEC monocultures(38). Therefore, the low VE-cadherin expression observed in Figure 2B for the HUVEC-only group is expected and supports the importance of co-culture or media supplementation in maintaining barrier function. By day 15, dextran permeability was highest in the ECGM2 + PSCM condition (1285.9 $\pm$ 119.0 pmol 4 kDa dextran/hr and 40.3 $\pm$ 6.7 pmol 65 kDa dextran/hr), similar to what was observed in the coculture study with PSCs, suggesting that PSCM media alone can cause vascular disfunction (**Figure 2DE**). Interestingly, the ECGM2 + STM condition exhibited an increase in permeability from the day 6 control when assessed at day 15 of culture (713.0 $\pm$ 116.7 pmol 4 kDa dextran/hr and 22.8 $\pm$ 6.5 pmol 65 kDa dextran/hr), however not as much of an increase as was seen with the ECGM2 only condition (901.4 $\pm$ 91.8 pmol 4 kDa dextran/hr and 26.4 $\pm$ 5.09 pmol 65 kDa dextran/hr). As a result, between the three media conditions tested, culture of HUVECs in compartmentalized ECGM2 + STM conditions resulted in the lowest barrier degradation over time. This can possibly be explained by the presence of ROCK inhibitor Y27632 and cAMP activator forskolin in STM media, which have been shown to have protective effects on endothelial barrier permeability(39–41). Notably, forskolin is also recognized for its capacity to promote the differentiation of stem cells into endothelial-like cells, emphasizing the critical role of the cAMP signaling pathway in endothelial cell culture(42). In summary, media alone did not improve vessel function over time, this improvement is attributed to HUVEC coculture with STs, which may be secreting soluble factors that fortify the endothelial barrier. However, the ECGM2 + STM media configuration resulted in the least vascular barrier degradation over time.

Effects of pericytes on vascular barrier permeability

To study the effects of pericytes on feto-maternal transport, placenta-derived pericytes were introduced into our AngioPlate placental barrier system. *In vivo*, fetal pericytes provide support to the

Lab on a Chip Accepted Manuscript

View Article Online
DOI: 10.1039/D5LC00075K

Open Access Article. Published on 27 May 2025. Downloaded on 6/4/2025 8:36:13 AM.
This article is licensed under a Creative Commons Attribution 3.0 Unported Licence.

endothelial barrier, play a role in immune cell regulation and vascular development, and control blood flow through vessels(43,44). However, their function in the placenta has not yet been heavily researched. Further, it has yet to be shown that they can be beneficial to the vascular barrier when incorporated into *in vitro* placental vascular models(45). Given that none of these previous models included STs in their coculture designs(45,46) and that we showed that ST media and ST coculture help support the vascular barrier, we incorporated primary human placental pericytes (hPC-PL) as single cell suspensions into the fibrin gel of our AngioPlate coculture with the goal of studying their effects on the model. Our AngioPlate system allows to perform two types of barrier testing: (1) vascular barrier permeability, which measures the passage of fluorescently labeled particles through the HUVEC layer into the interstitial fibrin matrix during coculture and (2) total barrier permeability, which assesses the transport of particles across both the HUVEC and ST layers into the fetal compartments. Both these assays are performed during coculture, which allows us to determine individual cell layer permeability whilst maintaining cellular crosstalk, which is not possible which conventional Transwell systems. To evaluate vascular permeability, 4 kDa and 65 kDa dextran were added to the inlet and outlet wells of the model and allowed to diffuse across the vascular barrier under perfusion conditions for 1 hour (**Figure 3A-C**). The change in fluorescence intensity within the central fibrin compartment between t=0 and t=1 hour was used to quantify the amount of fluorescent dextran that permeated the vascular channel. A "no cell" control was included to demonstrate the unobstructed maximum diffusion through the fibrin gel, as well as a "ST only" control which would allow the isolation of the ST monolayer's influence on the placental barrier.

Although there was no significant difference in 65 kDa dextran diffusion in the no cell and the ST only conditions due to the absence of endothelial barrier in both (56.1 ± 5.2 pmol/hr and 56.1 ± 5.3 pmol/hr, respectively, **Figure 3B**), the smaller 4 kDa dextran showed marginally decreased diffusion through in the STs only condition (1268 ± 132 pmol/hr) when compared to the no cell control (1457 ± 74 pmol/hr, **Figure 3C**). This could be explained by the fact that the ST cells create a barrier between the media in the gel and the media above the ST cells, which can reduce the volume into which the 4 kDa dextran diffused. The presence of a ST monolayer therefore resulted in a different concentration gradient throughout the gel, which is the driving factor in diffusion. As expected, 65 kDa dextran diffusion was much lower in all three vascularized conditions (3.4 ± 1.7 pmol/hr for STs + HUVECs, 9.0 ± 1.5 pmol/hr for STs + HUVECs + hPC-PL (high) and 5.8 ± 1.7 pmol/hr for STs + HUVECs + hPC-PL (low)), however the addition of pericytes did not have any effects on vascular permeability of this larger dextran.

In the case of 4 kDa dextran, the vascularized conditions once against exhibited lower permeabilities (195.9 ± 14.7 pmol/hr for STs + HUVECs, 440.4 ± 92.9 pmol/hr for STs + HUVECs + hPC-PL (high) and 317.4 ± 54.5 pmol/hr for STs + HUVECs + hPC-PL (low)). Interestingly, the addition of a higher density of pericytes increased the permeability of the vascular channel to 4 kDa dextran when compared to the ST+HUVEC condition. However, because this increase was small and was not paralleled in the 65 kDa dextran experiment, it is implied that the changes in transplacental permeability were minimal. To investigate the specific contribution of pericytes to vascular integrity independently of ST influence, we performed an additional experiment in which pericytes were cocultured with GFP-HUVECs alone. In this setup, we observed that pericytes enhanced vascular barrier integrity, supporting their known role in stabilizing and supporting microvasculature (**Figure S4**).

The increased permeability observed in the ST + HUVEC + hPC-PL (high) condition may be attributed to pericyte-induced matrix degradation or excessive cell proliferation, potentially leading to nutrient and oxygen depletion within the culture. This overgrowth may have been driven by the presence of PSC media supplements or by interactions with the STs. Thus, further optimization of culture conditions is needed to support the inclusion of a third cell type in this model. Alternatively, the lack of an observed barrier-

Lab on a Chip Accepted Manuscript

View Article Online
DOI: 10.1039/D5LC00075K

enhancing effect from pericytes may reflect a ceiling effect, where the STs already provided maximal support to the vasculature, leaving little room for further improvement.

Effects of pericytes on total barrier permeability

Once vascular permeability was assessed, the permeability of the entire placental barrier was evaluated (**Figure 3D-F**). As expected, the no cell control exhibited the highest permeation of both dextran types (197.5 ± 30.2 pmol/day for 4 kDa and 38.3 ± 5.9 pmol/day for 65 kDa dextran) and the three vascularized tissues exhibited the lowest 65 kDa dextran permeability (4.9 ± 0.8 pmol/day for ST + HUVECs, 4.5 ± 0.5 pmol/day for ST + HUVECs + hPC-PL (high) and 5.0 ± 0.8 pmol/day for ST + HUVECs + hPC-PL (low)) and no significant differences amongst them (**Figure 3EF**), similar to the vascular permeability assay (**Figure 3BC**). The ST only condition's permeability was significantly higher (11.0 ± 0.6 pmol/day) which could be explained by there being one cell barrier for the dextran to permeate through as opposed to the two in the vascularized models. Interestingly, there was no difference between 4 kDa dextran permeabilities in all four cell conditions. However, the ST+HUVEC condition (31.8 ± 5.7 pmol/day) trended towards being significantly different from the ST only condition (60.5 ± 8.0 pmol/day) and the two conditions containing pericytes (57.8 ± 17.0 pmol/day for high density and 57.5 ± 19.8 pmol/day for low density, respectively). Considering that the pericytes offered no improvement to vascular or total barrier permeability and that their overgrowth in the culture resulted in the overtaking of the vascular channel in some tissues and likely caused a reduction of nutrient availability for the endothelial and trophoblast cells, pericytes were not included in any future placental AngioPlate cultures.

Open Access Article. Published on 27 May 2025. Downloaded on 6/4/2025 8:36:13 AM.
This article is licensed under a Creative Commons Attribution 3.0 Unported Licence.

Lab on a Chip Accepted Manuscript

View Article Online
DOI: 10.1039/D5LC00075K

Open Access Article. Published on 27 May 2025. Downloaded on 6/4/2025 8:36:13 AM.
This article is licensed under a Creative Commons Attribution 3.0 Unported Licence.

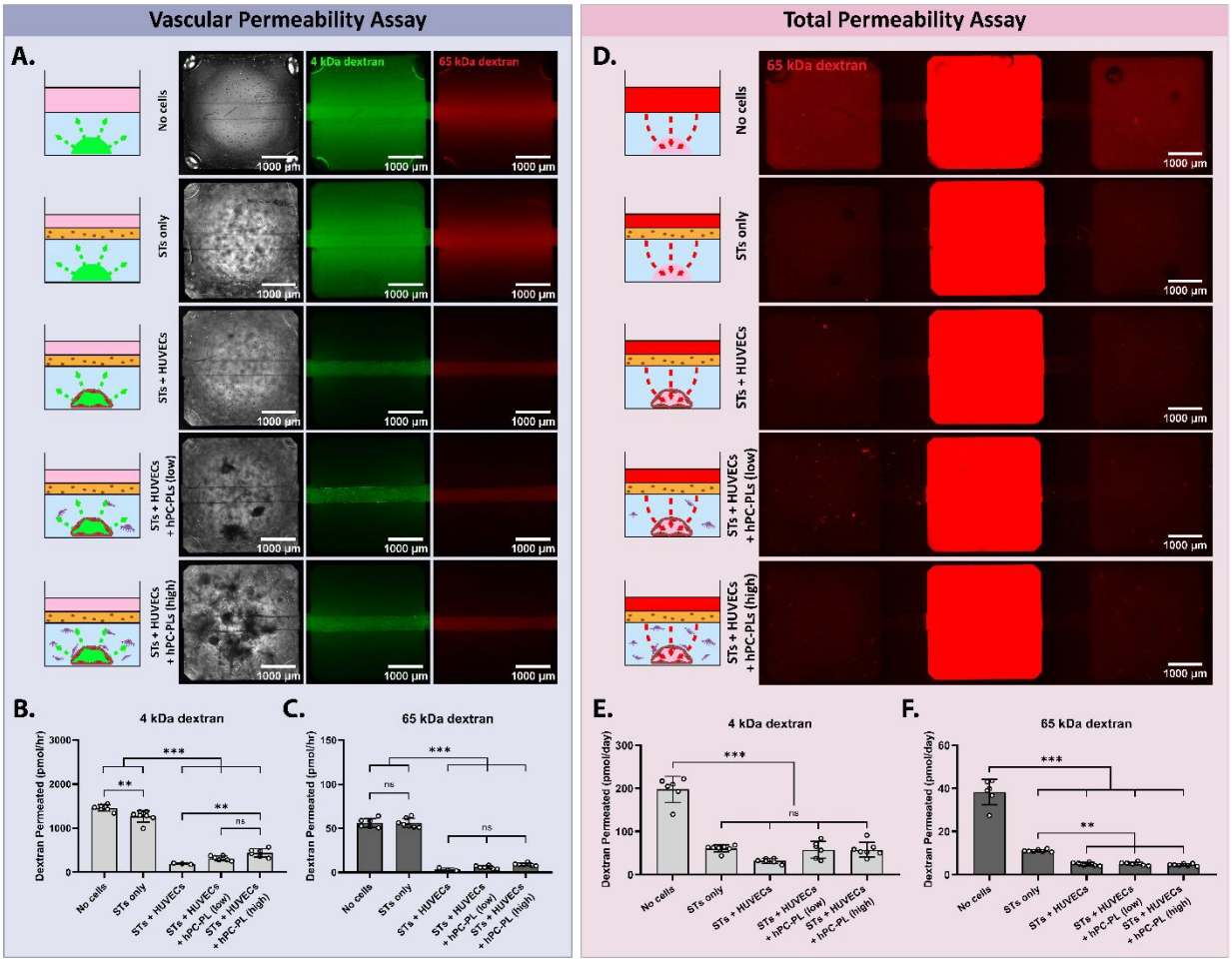

Figure 3. *Effects of pericytes on vascular and total permeability of placental barrier model on days 16 and 18 of culture.* ***A.*** *Brightfield images of vascular channel for the following conditions: no cell control, ST only, ST + HUVECs, and two tricultures with ST + HUVECs + hPC-Pls at high and low density. Fluorescent images of 4kDa (green) and 65 kDa (red) dextran permeation through endothelial channel after 1 hour of perfusion.* ***B.*** *Vascular barrier permeability to 4 kDa dextran. (N=3-7, one-way ANOVA, *p<0.05, **p<0.01, ***p<0.001)* ***C.*** *Vascular barrier permeability to 65 kDa dextran. (N=3-7, one-wayANOVA, *p<0.05, **p<0.01, ***p<0.001)* ***D.*** *Fluorescent images of 65 kDa dextran (red) permeating from the central maternal compartment, through the ST and HUVEC barriers, to the adjacent fetal compartments after 24 hours.* ***E.*** *Total barrier permeability to 4 kDa dextran from the maternal to the fetal compartments. (N=6-7, one-wayANOVA, **p<0.01, ***p<0.001)* ***F.*** *Total barrier permeability to 65 kDa dextran from the maternal to the fetal compartments. (N=6-7, one-wayANOVA, ***p<0.001)*

Drug barrier study

To assess the suitability of our platform with drug transport studies, we determined the permeability of our barrier system to three therapeutic agents: paclitaxel, a chemotherapeutic drug that triggers mitotic arrest and apoptosis in cancer cells(47), vancomycin, an antibiotic mainly prescribed to treat gram-positive bacterial infections(48), and immunoglobulin G from human serum, which is used in a variety of therapeutic strategies for patients with primary antibody deficiencies(49,50). These drugs were selected because of their known transport profiles supported by *in vivo* data and because they span the range of small molecules to large proteins. Fluorescently labeled versions of these drugs were introduced into the central maternal compartment of the device and incubated for 24 hours with vascular perfusion, before fetal concentrations were analyzed via fluorescent intensity measurement. A similar assay was also

Lab on a Chip Accepted Manuscript

View Article Online
DOI: 10.1039/D5LC00075K

performed with fluorescently labeled dextrans (4 kDa and 65 kDa) to isolate the effects of molecular size on permeability.

Breast cancer is the most common cancer type diagnosed during pregnancy, representing 40% of all cancer diagnoses, followed by lymphoma (12%) and cervical cancer (10%)(51). It has been shown that paclitaxel and other taxane therapies are a viable option for women suffering from cancer during pregnancy(52–54). Paclitaxel concentrations of 5 µM, 500 nM and 50 nM were introduced into the central maternal compartment. As expected, paclitaxel permeation into the fetal compartment was proportional to paclitaxel concentrations in the maternal media. Values ranged from 10.1 ± 3.4 pmol/day for the 5 µM maternal values to 0.3 ± 0.1 pmol/day for 500 nM, and values were out of range (OOR) for 50 nM (**Figure 4A**). This same downward trend was observed in the paclitaxel fetal-maternal ratios (F/M) (1.0 ± 0.3% for 5 µM, 0.3 ± 0.1% for 500 nM, OOR for 50 nM), suggesting a diffusion-driven permeation that is dependent on concentration gradients (**Figure 4E**). In comparison, Nekhayeva *et al.* perfused the maternal artery of 7 placental explants with 100 nM of paclitaxel for 2 hours and showed that the concentration of paclitaxel in the fetal circuit were also low at 4.3 ± 2.2 %(55) (**Figure 4G**). Similarly, a baboon study showed that fetal paclitaxel levels paralleled maternal concentrations at rates 100 times lower and the drug was not detectable in the fetal tissues at necropsy(56).

Vancomycin is an antibiotic drug commonly prescribed to treat serious bacterial infection during pregnancy. It has been confirmed to cross the placental barrier and to cause significant changes in the fetal microbiome and kidney injury in animal studies(8,57), however has not been shown to cause adverse effects during human pregnancy(2). Three vancomycin solutions were prepared at concentrations of 5 µg/ml, 500 ng/ml and 50 ng/ml and introduced into the maternal well. Similarly, vancomycin levels in the fetal compartment correlated to those in the maternal compartment with 41.6 ± 10.5 ng/day for a maternal concentration 5 µg/ml, 5.0 ± 0.5 ng/day for 500 ng/ml, 2.1 ± 0.6 ng/day for 50 ng/ml (**Figure 4B**). However, an inverse correlation between F/M values and maternal vancomycin concentrations were observed (4.2 ± 1.1% for 5 µg/ml of maternal vancomycin, 5.0 ± 0.5% for 500 ng/ml, 20.7 ± 6.2% for 50 ng/ml), suggesting that the transport of this antibiotic across the placental barrier may be transport-driven (**Figure 4E**). Further, although vancomycin and paclitaxel have similar molecular weights, their transport rates and F/M ratios differ significantly. This indicates that drug transport is influenced, at least to some extent, by the trophoblast layer, rather than occurring solely through simple diffusion. The vancomycin F/M ratios obtained in this study are consistent with those reported in ex vivo placental perfusion experiments(58,59). For instance, Nanovskaya et al. perfused placental explants with 25 µg/mL of vancomycin for 4 hours, observing a final F/M percentage of 9.6 ± 4% in the fetal circulation(59) (**Figure 4G**). Interestingly, in vivo studies measuring cord blood vancomycin concentrations in pregnant women have shown that fetal vancomycin levels can eventually reach maternal concentrations during maternal antibiotic infusions(60–62). Notably, these in vivo permeability values are higher than those observed in in vitro or ex vivo barrier models(58). It has been suggested that the presence of heparin in the media used for in vitro and ex vivo studies may lead to the formation of a heparin-vancomycin complex(58), which reduces the transplacental passage of vancomycin. In the present study, heparin, present in ECGM2 at concentrations higher than those in maternal blood, may have contributed to the reduced passive diffusion of vancomycin across the placental model.

The permeability of immunoglobulin G (IgG) from human serum was assessed at a maternal concentration of 1 mg/mL, revealing a transport rate across the placental barrier of 0.5 ± 0.2 µg/day, corresponding to F/M percentage of 0.3 ± 0.1% (**Figure 4C**). As anticipated, the transfer of IgG into the fetal compartment was significantly lower compared to smaller molecules such as dextrans, paclitaxel,

Open Access Article. Published on 27 May 2025. Downloaded on 6/4/2025 8:36:13 AM.
This article is licensed under a Creative Commons Attribution 3.0 Unported Licence.

Lab on a Chip Accepted Manuscript

View Article Online
DOI: 10.1039/D5LC00075K

Open Access Article. Published on 27 May 2025. Downloaded on 6/4/2025 8:36:13 AM.
This article is licensed under a Creative Commons Attribution 3.0 Unported Licence.

and vancomycin, primarily due to its larger size, which restricts passive diffusion. Beyond passive diffusion, IgG transport is facilitated by neonatal Fc receptors (FcRn) expressed on the ST surface, enabling selective antibody transport, with a preference hierarchy of IgG1 > IgG3 > IgG4 > IgG2(63). Clements et al. conducted a meta-analysis of 17 studies measuring maternal and cord IgG levels at birth, demonstrating that F/M ratios can exceed 1.0 by term due to months of active antibody transport(64). This contrasts with the lower F/M ratios observed in this study, which reflect only 24 hours of experimental conditions. In our previous work, we confirmed FcRn expression in STs through analysis of the FCGRT gene and found it to be comparable to levels in BeWo b30 cells(13), which are known to possess functional FcRn receptors(65). To further verify the presence of these receptors, future experiments could incorporate FcRn localization staining and inhibitor treatments to validate their role in antibody transport. In contrast, ex vivo placental perfusion studies have reported F/M IgG ratios comparable to those observed in our experiments (**Figure 4EF**). For instance, Malek et al. demonstrated that IgGs cross into the fetal compartment at approximately 0.5% of maternal concentrations after 6 hours of perfusion(66). Similarly, Miller et al. observed a fetal concentration of 0.6 ± 0.3% of the maternal IgG1 antibody I-F105 following a 6-hour perfusion(67). These findings reinforce the notion that IgG transfer across the placenta in ex vivo models is limited over short experimental time frames due to the highly selective and time-dependent nature of FcRn-mediated transport.

To assess the impact of size on barrier permeability and to elucidate the cumulative barrier effects the ST and EC barriers, we employed 4 kDa and 65 kDa dextrans (**Figure 4D**), which are considered relatively inert to mammalian cells(68), in a similar fluorescence-based assay. Permeabilities to 65 kDa dextran were statistically similar for the single layer HUVECs only conditions (4.7 ± 1.4 pmol/day) and the double layer STs + HUVECs condition (2.6 ± 1.1 pmol/day), but much lower than the no cell control (31.2 ± 3.0 pmol/day). This suggests that the HUVEC barrier is so minimally permeable to 65 kDa that the extra ST layer has no discernible effect, which agrees with previous findings of HUVEC dextran permeability(69). When converting the 65 kDa dextran permeability rate of the ST + HUVEC condition to a F/M ratio, we obtain a value of 0.4 ± 0.2%, which is higher but in in the same order of magnitude as that of IgG (0.3 ± 0.1%, **Figure 4E**). This can be explained by the fact that these molecules are of similar sizes, with IgGs averaging a higher molecular weight of 150 kDa(70). In contrast, the smaller 4 kDa dextran permeated the STs + HUVECs barrier (37.3 ± 6.0 pmol/day) at a lower rate than the HUVEC only culture (45.6 ± 7.5 pmol/day), due to the fact that the endothelial layer is semi-permeable to smaller dextrans(69). The fetal/maternal ratios of 4 kDa dextran in the ST + HUVEC coculture equate to 6.1 ± 1.0%, which is closer the that of smaller molecules such as vancomycin (4.2 ± 1.1% for 5 µg/ml of maternal vancomycin, 5.0 ± 0.5% for 500 ng/ml, 20.7 ± 6.2% for 50 ng/ml). In summary, these findings confirm that the permeability of our placental barrier model is molecule size, concentration, as well as drug-type dependent and can therefore be used to explore the safety of many commonly prescribed medications during pregnancy.

Lab on a Chip Accepted Manuscript

View Article Online
DOI: 10.1039/D5LC00075K

Open Access Article. Published on 27 May 2025. Downloaded on 6/4/2025 8:36:13 AM.
This article is licensed under a Creative Commons Attribution 3.0 Unported Licence.

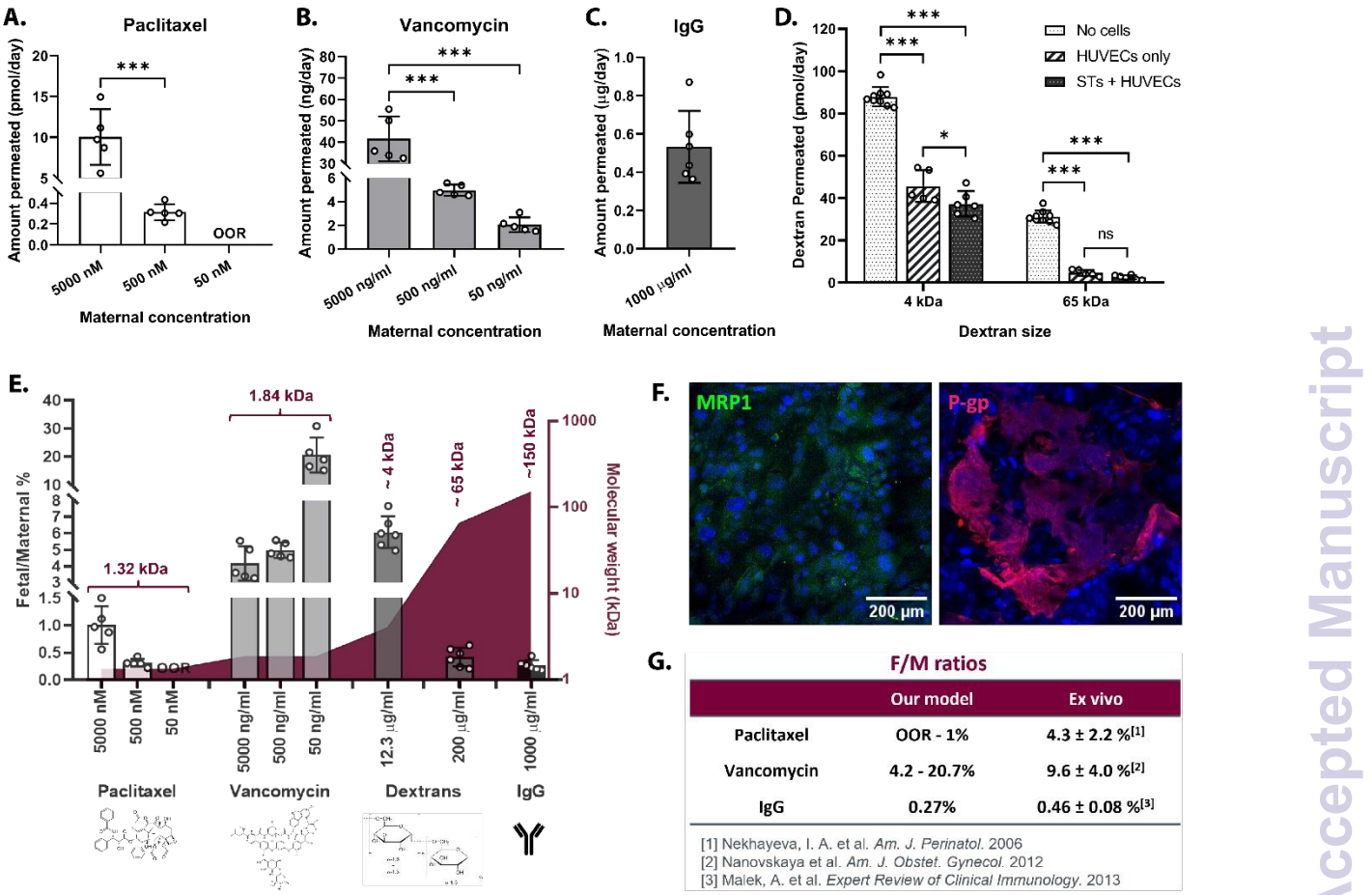

Figure 4. *Drug permeability of AngioPlate placental barrier model.* ***A.-C.*** *Permeation of paclitaxel, vancomycin and immunoglobulin G from the maternal compartment to the fetal compartment after 24 hrs of vascular perfusion. OOR: Out of Range. (N=5, one-way ANOVA, *p<0.0, **p<0.01, ***p<0.001)* ***D.*** *Total barrier permeability to 4 kDa and 65 kDa dextrans from the maternal to the fetal compartments in no cell, HUVEC only and STs + HUVECs conditions. (N=5, one-way ANOVA, *p<0.0, **p<0.01, ***p<0.001)* ***E.*** *Fetal to maternal (F/M) ratios of drugs and dextrans after 24 hours of vascular perfusion at different molecular concentrations. Secondary y-axis displays the molecular weight of the fluorescently labeled molecules. (N=5-6)* ***F.*** *Immunofluorescent staining of drug transporters in the ST monolayer of the placental barrier model. MRP1 is shown in green and P-gp in red, highlighting their expression and localization within the syncytiotrophoblast layer.* ***G.*** *F/M ratios of ex vivo placental explants for paclitaxel(55), vancomycin(59) and IgG(71) from human serum.*

Lab on a Chip Accepted Manuscript

View Article Online
DOI: 10.1039/D5LC00075K

Open Access Article. Published on 27 May 2025. Downloaded on 6/4/2025 8:36:13 AM.
This article is licensed under a Creative Commons Attribution 3.0 Unported Licence.

Discussion

The placenta serves as the primary site of exchange between the mother and fetus, making it a key focus of studies aimed at understanding which xenobiotic compounds can cross into the fetal circulation. In this work, we designed a scalable placental barrier model consisting of a ST layer separating the maternal compartment from the model fetal vessel. Primary CTs cells have long been regarded as the gold standard for *in vitro* human placental cultures due to their genetic similarity to *in vivo* tissues. However, they present significant challenges, including limited accessibility, demanding maintenance requirements, and the potential for spontaneous differentiation. The trophoblast stem cells and differentiation protocol used in this paper were established by Okae *et al.* and have achieved large-scale popularity in *in vitro* placental modeling due to their capacity to differentiate into a highly-fused syncytium(14). In our previous work, we compared the differentiation capacity of these stem cells to the model choriocarcinoma cell line BeWo b30 by evaluating their fusion percentage, hCG secretion rates, polarity, morphology and gene expression(13). We determined that the stem cells were immensely better at differentiating into STs and they have since become the cell type of choice for our models.

In this current placental barrier model, we first evaluated the effects of ST coculture on the endothelial vasculature, as well as the effects of the corresponding mixed coculture medium. We found that the ST cells assumed a protective role for the endothelial culture by secreting pro-angiogenic factors that support vascular growth. Leptin and PLGF levels in the device's media supernatant were drastically increased by 171.2- and 2.1-fold, respectively, with the addition of trophoblasts to the system. This coincided with an improvement in vascular channel integrity, decreased vessel leakiness and stronger staining of ve-cadherin. These findings align with previous studies investigating the roles of leptin and PLGF both *in vivo* and *ex vivo* endothelium. PlGF has been shown to strongly activate the ERK1/2 pathway in endothelial cells, which controls cell proliferation, angiogenesis, vascular permeability and response to hypoxic stress (72,73). For example, Chau *et al.* showed that treatment with PlGF increased cell proliferation under hypoxic conditions for both trophoblast and endothelial cells(74). Similarly, leptin has been shown to have strong angiogenic effects in vivo and in vitro(75). Although the effects that these pro-angiogenic cytokines have on endothelial cells have been widely studied, this study is the first to investigate how the inclusion of trophoblasts influences vascular permeability to small molecules. In addition to driving the secretion of angiogenic cytokines ST layers reached confluence faster when cocultured with endothelial cells, suggesting a possible positive feedback loop between ST and endothelial cells.

Another key point in this study was to evaluate the effects of incorporating placental pericytes into the model on barrier effectiveness. Pericytes are known to direct branching angiogenesis and control blood flow rates in other human organs(76), however, their function in the human placenta has not been extensively explored. Interestingly, pericytes preferentially cover endothelial junctions furthest away from the trophoblast layer(77), suggesting that trophoblast-pericyte crosstalk modulates pericyte localization in the placenta. In this study, we demonstrated that the presence of pericytes in our placental barrier model did not enhance barrier integrity, which led to their exclusion from the final model. However, Haase *et al.* showed that the addition of placental pericytes was detrimental to their placental microvascular model because they triggered preeclampsia-associated cytokine production, inhibited vascular grown and caused microvascular leakage(45). The authors attributed this to an imbalance in endothelial-pericyte communication, more specifically a disruption of signaling through the VEGF-Ang-Tie2 pathway, demonstrating the importance of the optimization of these types of cocultures.

Lab on a Chip Accepted Manuscript

View Article Online
DOI: 10.1039/D5LC00075K

Open Access Article. Published on 27 May 2025. Downloaded on 6/4/2025 8:36:13 AM.
This article is licensed under a Creative Commons Attribution 3.0 Unported Licence.

In this work we quantified transport of three drug across our placental barrier and compared the fetal/maternal permeation rates to those reported from ex vivo cultures. Fluorescently-labelled paclitaxel, vancomycin, dextran and IgG were selected to span both the size and types of molecules that may be transported into the fetal bloodstream. These molecules traverse the placental barrier through various mechanisms, including passive diffusion, facilitated diffusion, active transport, exocytosis/endocytosis, and transporter proteins(78). The transport profiles observed will typically reflect the specific transport mechanisms associated with each type of molecule.

Paclitaxel is often prescribed as a cancer treatment during pregnancy because it transfers to the fetus at concentrations below 5% of those found in maternal circulation. This limited transfer is primarily due to the efflux transporter P-glycoprotein (P-gp), which actively transports paclitaxel—and other substances such as antibiotics, steroids, and protease inhibitors—back into the maternal circulation from placental cells. Consequently, this mechanism effectively reduces fetal exposure to these compounds. In our previous work, we showed that our STs express P-gp at similar rates as BeWo b30, which have known to express these functional transporters(79). In the current study, we further confirmed the presence of P-gp in the AngioPlate model by performing MDR1 immunostaining, as shown in **Figure 4F**. We also stained for MRP1, another key efflux transporter involved in placental drug resistance and observed robust expression in the ST monolayer (**Figure 4F**), further supporting the model's physiological relevance. Our permeability data (**Figure 4AE**) demonstrates that as paclitaxel concentrations in the maternal bloodstream increase, so too do the concentrations in the fetal bloodstream, highlighting this transport dynamic. A similar trend was observed with the fetal concentrations of vancomycin (**Figure 4BE**), which is of a similar size to paclitaxel and is primarily transported across the placenta via passive diffusion. When this data is converted to fetal/maternal ratios, we observed lower F/M ratios for paclitaxel, which can be explained by the presence of P-gp efflux transporters actively removing large concentrations of paclitaxel molecules from the placental cells. The dextrans, which are also transported across the placenta via passive diffusion, had fetal concentrations and F/M ratios reflective of their size. 4 kDa dextran had F/M ratios similar to those of vancomycin (**Figure 4E**), which has a molecular weight of 1.84 kDa, whereas the 65 kDa dextran has much lower F/M ratios given the larger molecule size will cause steric hindrance during passive diffusion. IgGs which have an average molecular weight of 150 kDa crossed the placental barrier at even lower F/M rates, as expected. This new transporter characterization supports the relevance of our model for studying both passive and active mechanisms of drug transport across the placental barrier. When expanding the list of drugs tested on this model it could be beneficial to identify the localization of certain transporters to thus associate the quantity of drug permeation to the transport type.

The PSCs used in this work were first developed in 2018 by Okae *et al.* from blastocyst and CT-derived cells(14), however, to create a large library of PSCs from patients with diverse genetic backgrounds, regular access to human embryos and first-trimesters placentas would be required using this protocol. To address this, Castel *et al.* developed a cellular reprogramming protocol starting with adult human somatic or pluripotent cells and resulting in induced trophoblast stem cells akin to post-implantation 8-10 day CTs(80). Using an adapted Okae differentiation protocol, these induced trophoblast stem cells were successfully differentiated into both STs and EVTs, showcasing a promising approach for placental research with patient-derived cells.

Many placental organoid model systems have since been developed using this cell type or using their differentiation protocol(80–85). In fact, this protocol has been applied to generate differentiated trophoblast organoids from both patient-derived somatic cells and induced pluripotent stem cells(80–82). However, most post-culture analyses focused primarily on genetic sequencing and localized marker expression, with minimal inclusion of functional assays or detailed organoid characterization. However,

Lab on a Chip Accepted Manuscript

View Article Online
DOI: 10.1039/D5LC00075K

Open Access Article. Published on 27 May 2025. Downloaded on 6/4/2025 8:36:13 AM.
This article is licensed under a Creative Commons Attribution 3.0 Unported Licence.

even the most complex placental organoid models suffer from incompatibility with permeability testing given the inaccessibility of their central compartment. In our AngioPlate placental model, not only can we perform barrier testing, but we have the ability to separately assess the permeability of the vascular channel or the syncytial barrier (vascular permeability assay vs total permeability assay) during coculture, which is not possible using conventional Transwell systems. For total permeability analysis, this functional assay is highly scalable, facilitating high-throughput drug screening by quantifying permeated drugs via mass spectrometry—a method particularly advantageous when fluorescently-tagged drugs are limited in availability. Further, the composition of the model's fibrin hydrogel matrix is compatible with protein and RNA extraction methods, as shown in our previous work(13). In fact, Carrion *et el.* showed that the fibrinolytic protease nattokinase has the capacity to cleave fibrin bonds within a cell-laden fibrin hydrogel to obtain a single cell suspension(86). The resulting samples can then be used for downstream applications of proteomics or gene sequencing. Given the important advantages of these systems, chip and plate-based models will remain the standard for *in vitro* placental transport studies.

Conclusion

High fidelity *in* vitro placental barrier models are necessary to determine the safety of prescription drugs regimes during pregnancy. In this work, we engineered a 3D placental barrier model that incorporates both differentiated ST and endothelial layers and is compatible with the high-throughput requirements of drug safety assays. Once the coculture model was established, we showed that the ST cells and their media perform a supportive role in maintained vascular barrier integrity over 18 days in culture, allowing for efficient syncytial differentiation of the trophoblasts, which is vital to term placental modeling. This extended culture time offers the opportunity for longer drug treatment studies in future work. Finally, when assessing the permeability of three drug types (chemotherapeutics, antibiotics, and antibodies) we determined that the barrier permeability was molecule, size, type and concentration dependent, agreeing with in vivo and ex vivo literature findings.

Acknowledgements

This work was made possible by the financial support of the Natural Sciences and Engineering Research Council of Canada (NSERC) Discovery Grant (RGPIN-05500-2018) and Canadian Institute of Health Research (CIHR) Project Grant (PJT-166052) to B.Z. The authors are grateful to the contributors to BioRender.com which was used to make the illustrations in this work. The authors would like to thank Justin Bernar from the Chemical Engineering Department Machine Shop at McMaster University for his help milling all the plates used in this work.

Author Contributions

S.K. performed the experiments, analyzed the results, and prepared the manuscript. P.S. assisted with the design and manufacturing of AngioPlates. M.L. contributed to stem cell culture and immunostaining. B.Z. envisioned the concept, supervised the work and edited the manuscript.

Competing Interests

B.Z. holds equities in OrganoBiotech, Inc. which is commercializing the AngioPlate Platform used in this work.

Lab on a Chip Accepted Manuscript

View Article Online
DOI: 10.1039/D5LC00075K

Open Access Article. Published on 27 May 2025. Downloaded on 6/4/2025 8:36:13 AM.
This article is licensed under a Creative Commons Attribution 3.0 Unported Licence.

References

1. Werler MM, Kerr SM, Ailes EC, Reefhuis J, Gilboa SM, Browne ML, et al. Patterns of Prescription Medication Use during the First Trimester of Pregnancy in the United States, 1997–2018. Clin Pharmacol Ther. 2023;114(4):836–44.

2. Bookstaver PB, Bland CM, Griffin B, Stover KR, Eiland LS, McLaughlin M. A Review of Antibiotic Use in Pregnancy. Pharmacother J Hum Pharmacol Drug Ther. 2015;35(11):1052–62.

3. Creeley CE, Denton LK. Use of Prescribed Psychotropics during Pregnancy: A Systematic Review of Pregnancy, Neonatal, and Childhood Outcomes. Brain Sci. 2019 Sep;9(9):235.

4. Rampono J, Simmer K, Ilett KF, Hackett LP, Doherty DA, Elliot R, et al. Placental Transfer of SSRI and SNRI Antidepressants and Effects on the Neonate. Pharmacopsychiatry. 2009 May;42(3):95–100.

5. Meng LC, Lin CW, Chuang HM, Chen LK, Hsiao FY. Benzodiazepine Use During Pregnancy and Risk of Miscarriage. JAMA Psychiatry [Internet]. 2023 Dec 27 [cited 2024 Mar 6]; Available from: https://doi.org/10.1001/jamapsychiatry.2023.4912

6. van Hove H, Mathiesen L, Freriksen JJM, Vähäkangas K, Colbers A, Brownbill P, et al. Placental transfer and vascular effects of pharmaceutical drugs in the human placenta *ex vivo*: A review. Placenta. 2022 May 1;122:29–45.

7. Nahum GG, Uhl K, Kennedy DL. Antibiotic Use in Pregnancy and Lactation: What Is and Is Not Known About Teratogenic and Toxic Risks. Obstet Gynecol. 2006 May;107(5):1120.

8. Alhasan MM, Cait AM, Heimesaat MM, Blaut M, Klopfleisch R, Wedel A, et al. Antibiotic use during pregnancy increases offspring asthma severity in a dose-dependent manner. Allergy. 2020;75(8):1979–90.

9. Esposito S, Tenconi R, Preti V, Groppali E, Principi N. Chemotherapy against cancer during pregnancy. Medicine (Baltimore). 2016 Sep 23;95(38):e4899.

10. Daw JR, Hanley GE, Greyson DL, Morgan SG. Prescription drug use during pregnancy in developed countries: a systematic review. Pharmacoepidemiol Drug Saf. 2011;20(9):895–902.

11. Wesley BD, Sewell CA, Chang CY, Hatfield KP, Nguyen CP. Prescription medications for use in pregnancy–perspective from the US Food and Drug Administration. Am J Obstet Gynecol. 2021 Jul 1;225(1):21–32.

12. Cherubini M, Erickson S, Haase K. Modelling the Human Placental Interface In Vitro—A Review. Micromachines. 2021 Aug;12(8):884.

13. Kouthouridis S, Sotra A, Khan Z, Alvarado J, Raha S, Zhang B. Modeling the Progression of Placental Transport from Early- to Late-Stage Pregnancy by Tuning Trophoblast Differentiation and Vascularization. Adv Healthc Mater. 2023;12(32):2301428.

Lab on a Chip Accepted Manuscript

View Article Online
DOI: 10.1039/D5LC00075K

Open Access Article. Published on 27 May 2025. Downloaded on 6/4/2025 8:36:13 AM.
This article is licensed under a Creative Commons Attribution 3.0 Unported Licence.

14. Okae H, Toh H, Sato T, Hiura H, Takahashi S, Shirane K, et al. Derivation of Human Trophoblast Stem Cells. Cell Stem Cell. 2018 Jan 4;22(1):50-63.e6.

15. Zhang F, Lin DSY, Rajasekar S, Sotra A, Zhang B. Pump-Less Platform Enables Long-Term Recirculating Perfusion of 3D Printed Tubular Tissues. Adv Healthc Mater. 2023;12(27):2300423.

16. Göttlicher M, Minucci S, Zhu P, Krämer OH, Schimpf A, Giavara S, et al. Valproic acid defines a novel class of HDAC inhibitors inducing differentiation of transformed cells. EMBO J. 2001 Dec 17;20(24):6969–78.

17. Zampetaki A, Zeng L, Margariti A, Xiao Q, Li H, Zhang Z, et al. Histone Deacetylase 3 Is Critical in Endothelial Survival and Atherosclerosis Development in Response to Disturbed Flow. Circulation. 2010 Jan 5;121(1):132–42.

18. Kashio T, Shirakura K, Kinoshita M, Morita M, Ishiba R, Muraoka K, et al. HDAC inhibitor, MS-275, increases vascular permeability by suppressing Robo4 expression in endothelial cells. Tissue Barriers. 2021 Jul 3;9(3):1911195.

19. Jaju Bhattad G, Jeyarajah MJ, McGill MG, Dumeaux V, Okae H, Arima T, et al. Histone deacetylase 1 and 2 drive differentiation and fusion of progenitor cells in human placental trophoblasts. Cell Death Dis. 2020 May 4;11(5):1–17.

20. Bala K, Ambwani K, Gohil NK. Effect of different mitogens and serum concentration on HUVEC morphology and characteristics: Implication on use of higher passage cells. Tissue Cell. 2011 Aug 1;43(4):216–22.

21. Margolis EA, Cleveland DS, Kong YP, Beamish JA, Wang WY, Baker BM, et al. Stromal Cell Identity Modulates Vascular Morphogenesis in a Microvasculature-on-a-Chip Platform. Lab Chip. 2021 Mar 21;21(6):1150–63.

22. Alimperti S, Mirabella T, Bajaj V, Polacheck W, Pirone DM, Duffield J, et al. Three-dimensional biomimetic vascular model reveals a RhoA, Rac1, and N-cadherin balance in mural cell–endothelial cell-regulated barrier function. Proc Natl Acad Sci. 2017 Aug 15;114(33):8758–63.

23. Grainger SJ, Carrion B, Ceccarelli J, Putnam AJ. Stromal Cell Identity Influences the In Vivo Functionality of Engineered Capillary Networks Formed by Co-delivery of Endothelial Cells and Stromal Cells. Tissue Eng Part A. 2013 May;19(9–10):1209–22.

24. Costa-Almeida R, Gomez-Lazaro M, Ramalho C, Granja PL, Soares R, Guerreiro SG. Fibroblast-Endothelial Partners for Vascularization Strategies in Tissue Engineering. Tissue Eng Part A. 2015 Mar 1;21(5–6):1055–65.

25. Lee JG, Yon JM, Kim G, Lee SG, Kim CY, Cheong SA, et al. PIBF1 regulates trophoblast syncytialization and promotes cardiovascular development. Nat Commun. 2024 Feb 19;15(1):1487.

26. Blunk T, Sieminski AL, Appel B, Croft C, Courter DL, Chieh JJ, et al. Bone Morphogenetic Protein 9: A Potent Modulator of Cartilage Development In Vitro. Growth Factors. 2003 Jan 1;21(2):71–7.

Lab on a Chip Accepted Manuscript

View Article Online
DOI: 10.1039/D5LC00075K

Open Access Article. Published on 27 May 2025. Downloaded on 6/4/2025 8:36:13 AM.
This article is licensed under a Creative Commons Attribution 3.0 Unported Licence.

27. Suzuki Y, Ohga N, Morishita Y, Hida K, Miyazono K, Watabe T. BMP-9 induces proliferation of multiple types of endothelial cells in vitro and in vivo. J Cell Sci. 2010 May 15;123(10):1684–92.

28. Solchaga LA, Penick K, Porter JD, Goldberg VM, Caplan AI, Welter JF. FGF-2 enhances the mitotic and chondrogenic potentials of human adult bone marrow-derived mesenchymal stem cells. J Cell Physiol. 2005;203(2):398–409.

29. Park DS, Park JC, Lee JS, Kim TW, Kim KJ, Jung BJ, et al. Effect of FGF-2 on Collagen Tissue Regeneration by Human Vertebral Bone Marrow Stem Cells. Stem Cells Dev. 2015 Jan 15;24(2):228–43.

30. Cao R, Eriksson A, Kubo H, Alitalo K, Cao Y, Thyberg J. Comparative Evaluation of FGF-2–, VEGF-A–, and VEGF-C–Induced Angiogenesis, Lymphangiogenesis, Vascular Fenestrations, and Permeability. Circ Res. 2004 Mar 19;94(5):664–70.

31. Mantzoros CS, Magkos F, Brinkoetter M, Sienkiewicz E, Dardeno TA, Kim SY, et al. Leptin in human physiology and pathophysiology. Am J Physiol-Endocrinol Metab. 2011 Oct;301(4):E567–84.

32. Bouloumié A, Drexler HCA, Lafontan M, Busse R. Leptin, the Product of Ob Gene, Promotes Angiogenesis. Circ Res. 1998 Nov 16;83(10):1059–66.

33. Maymó JL, Pérez Pérez A, Gambino Y, Calvo JC, Sánchez-Margalet V, Varone CL. Review: Leptin gene expression in the placenta – Regulation of a key hormone in trophoblast proliferation and survival. Placenta. 2011 Mar 1;32:S146–53.

34. Herrera-Vargas AK, García-Rodríguez E, Olea-Flores M, Mendoza-Catalán MA, Flores-Alfaro E, Navarro-Tito N. Pro-angiogenic activity and vasculogenic mimicry in the tumor microenvironment by leptin in cancer. Cytokine Growth Factor Rev. 2021 Dec 1;62:23–41.

35. Stürzebecher PE, Kralisch S, Schubert MR, Filipova V, Hoffmann A, Oliveira F, et al. Leptin treatment has vasculo-protective effects in lipodystrophic mice. Proc Natl Acad Sci. 2022 Oct 4;119(40):e2110374119.

36. Lash GE, Naruse K, Innes BA, Robson SC, Searle RF, Bulmer JN. Secretion of angiogenic growth factors by villous cytotrophoblast and extravillous trophoblast in early human pregnancy. Placenta. 2010 Jun;31(6):545–8.

37. Vrachnis N, Kalampokas E, Sifakis S, Vitoratos N, Kalampokas T, Botsis D, et al. Placental growth factor (PlGF): a key to optimizing fetal growth. J Matern Fetal Neonatal Med. 2013 Jul 1;26(10):995–1002.

38. Kosyakova N, Kao DD, Figetakis M, López-Giráldez F, Spindler S, Graham M, et al. Differential functional roles of fibroblasts and pericytes in the formation of tissue-engineered microvascular networks in vitro. Npj Regen Med. 2020 Jan 6;5(1):1–12.

39. Liu L, Jiang Y, Steinle JJ. Forskolin regulates retinal endothelial cell permeability through TLR4 actions in vitro. Mol Cell Biochem. 2021 Dec 1;476(12):4487–92.

40. Rokhzan R, Ghosh CC, Schaible N, Notbohm J, Yoshie H, Ehrlicher AJ, et al. Multiplexed, high-throughput measurements of cell contraction and endothelial barrier function. Lab Invest. 2019 Jan 1;99(1):138–45.

Lab on a Chip Accepted Manuscript

View Article Online
DOI: 10.1039/D5LC00075K

Open Access Article. Published on 27 May 2025. Downloaded on 6/4/2025 8:36:13 AM.
This article is licensed under a Creative Commons Attribution 3.0 Unported Licence.

41. van Nieuw Amerongen GP, Musters RJP, Eringa EC, Sipkema P, van Hinsbergh VWM. Thrombin-induced endothelial barrier disruption in intact microvessels: role of RhoA/Rho kinase-myosin phosphatase axis. Am J Physiol-Cell Physiol. 2008 May;294(5):C1234–41.

42. Yi B, Ding T, Jiang S, Gong T, Chopra H, Sha O, et al. Conversion of stem cells from apical papilla into endothelial cells by small molecules and growth factors. Stem Cell Res Ther. 2021 May 3;12(1):266.

43. Kandzija N, Rahbar M, Jones GD, Motta-Mejia C, Zhang W, Couch Y, et al. Placental capillary pericytes release excess extracellular vesicles under hypoxic conditions inducing a pro-angiogenic profile in term pregnancy. Biochem Biophys Res Commun. 2023 Apr 9;651:20–9.

44. Barreto RSN, Romagnolli P, Cereta AD, Coimbra-Campos LMC, Birbrair A, Miglino MA. Pericytes in the Placenta: Role in Placental Development and Homeostasis. In: Birbrair A, editor. Pericyte Biology in Different Organs [Internet]. Cham: Springer International Publishing; 2019 [cited 2024 Feb 13]. p. 125–51. (Advances in Experimental Medicine and Biology). Available from: https://doi.org/10.1007/978-3-030-11093-2_8

45. Haase K, Gillrie MR, Hajal C, Kamm RD. Pericytes Contribute to Dysfunction in a Human 3D Model of Placental Microvasculature through VEGF-Ang-Tie2 Signaling. Adv Sci. 2019;6(23):1900878.

46. Cherubini M, Haase K. A Bioengineered Model for Studying Vascular-Pericyte Interactions of the Placenta. In: Margadant C, editor. Cell Migration in Three Dimensions [Internet]. New York, NY: Springer US; 2023 [cited 2024 Feb 14]. p. 409–23. (Methods in Molecular Biology). Available from: https://doi.org/10.1007/978-1-0716-2887-4_23

47. Wang TH, Wang HS, Soong YK. Paclitaxel-induced cell death. Cancer. 2000;88(11):2619–28.

48. Walsh C. Deconstructing Vancomycin. Science. 1999 Apr 16;284(5413):442–3.

49. Gardulf A, Nicolay U. Replacement IgG therapy and self-therapy at home improve the health-related quality of life in patients with primary antibody deficiencies. Curr Opin Allergy Clin Immunol. 2006 Dec;6(6):434.

50. Gardulf A, Andersson E, Lindqvist M, Hansen S, Gustafson R. Rapid Subcutaneous IgG Replacement Therapy at Home for Pregnant Immunodeficient Women. J Clin Immunol. 2001 Mar 1;21(2):150–4.

51. Maggen C, Wolters VERA, Cardonick E, Fumagalli M, Halaska MJ, Lok CAR, et al. Pregnancy and Cancer: the INCIP Project. Curr Oncol Rep. 2020 Feb 5;22(2):17.

52. Cardonick E, Bhat A, Gilmandyar D, Somer R. Maternal and fetal outcomes of taxane chemotherapy in breast and ovarian cancer during pregnancy: case series and review of the literature. Ann Oncol Off J Eur Soc Med Oncol. 2012 Dec;23(12):3016–23.

53. Cardonick EH, O'Laughlin AE, So SC, Fleischer LT, Akoto S. Paclitaxel use in pregnancy: neonatal follow-up of infants with positive detection of intact paclitaxel and metabolites in meconium at birth. Eur J Pediatr. 2022 Apr 1;181(4):1763–6.

Lab on a Chip Accepted Manuscript

View Article Online
DOI: 10.1039/D5LC00075K

Open Access Article. Published on 27 May 2025. Downloaded on 6/4/2025 8:36:13 AM.
This article is licensed under a Creative Commons Attribution 3.0 Unported Licence.

54. Girardelli S, Bonomo B, Papale M, di Loreto E, Grossi E, Scarfone G, et al. Weekly Paclitaxel for Pregnancy Associated Breast Cancer. Clin Breast Cancer [Internet]. 2023 Dec 13 [cited 2024 Mar 6]; Available from: https://www.sciencedirect.com/science/article/pii/S1526820923003026

55. Nekhayeva IA, Nanovskaya TN, Hankins GDV, Ahmed MS. Role of Human Placental Efflux Transporter P-Glycoprotein in the Transfer of Buprenorphine, Levo-α-Acetylmethadol, and Paclitaxel. Am J Perinatol. 2006 Sep;23(7):423–30.

56. Calsteren KV, Verbesselt R, Devlieger R, De Catte L, Chai DC, Van Bree R, et al. Transplacental transfer of paclitaxel, docetaxel, carboplatin, and trastuzumab in a baboon model. Int J Gynecol Cancer Off J Int Gynecol Cancer Soc. 2010 Dec;20(9):1456–64.

57. Joshi MD, Pais GM, Chang J, Hlukhenka K, Avedissian SN, Gulati A, et al. Evaluation of Fetal and Maternal Vancomycin-Induced Kidney Injury during Pregnancy in a Rat Model. Antimicrob Agents Chemother. 2019 Sep 23;63(10):10.1128/aac.00761-19.

58. Hnat MD, Gainer J, Bawdon RE, Wendel GD. Transplacental passage of vancomycin in the ex vivo human perfusion model. Infect Dis Obstet Gynecol. 2004;12(2):57–61.

59. NANOVSKAYA T, PATRIKEEVA S, ZHAN Y, FOKINA V, HANKINS GD, AHMED MS. Transplacental transfer of vancomycin and telavancin. Am J Obstet Gynecol. 2012 Oct;207(4):331.e1-331.e6.

60. Laiprasert J, Klein K, Mueller BA, Pearlman MD. Transplacental passage of vancomycin in noninfected term pregnant women. Obstet Gynecol. 2007 May;109(5):1105–10.

61. Onwuchuruba CN, Towers CV, Howard BC, Hennessy MD, Wolfe L, Brown MS. Transplacental passage of vancomycin from mother to neonate. Am J Obstet Gynecol. 2014 Apr 1;210(4):352.e1-352.e4.

62. Towers CV, Weitz B. Transplacental passage of vancomycin. J Matern Fetal Neonatal Med. 2018 Apr 18;31(8):1021–4.

63. Wessel RE, Dolatshahi S. Quantitative mechanistic model reveals key determinants of placental IgG transfer and informs prenatal immunization strategies. PLOS Comput Biol. 2023 Nov 7;19(11):e1011109.

64. Clements T, Rice TF, Vamvakas G, Barnett S, Barnes M, Donaldson B, et al. Update on Transplacental Transfer of IgG Subclasses: Impact of Maternal and Fetal Factors. Front Immunol [Internet]. 2020 [cited 2020 Nov 15];11. Available from: https://www.frontiersin.org/articles/10.3389/fimmu.2020.01920/full

65. Xu Y, He Y, Momben-Abolfath S, Vertrees D, Li X, Norton MG, et al. Zika Virus Infection and Antibody Neutralization in FcRn Expressing Placenta and Engineered Cell Lines. Vaccines. 2022 Dec;10(12):2059.

66. Malek A, Sager R, Zakher A, Schneider H. Transport of immunoglobulin G and its subclasses across the in vitro-perfused human placenta. Am J Obstet Gynecol. 1995 Sep 1;173(3):760–7.

Lab on a Chip Accepted Manuscript

View Article Online
DOI: 10.1039/D5LC00075K

Open Access Article. Published on 27 May 2025. Downloaded on 6/4/2025 8:36:13 AM.
This article is licensed under a Creative Commons Attribution 3.0 Unported Licence.

67. Miller RK, Mace K, Polliotti B, DeRita R, Hall W, Treacy G. Marginal Transfer of ReoPro™ (Abciximab) Compared with Immunoglobulin G (F105), Inulin and Water in the Perfused Human Placenta In Vitro. Placenta. 2003 Aug 1;24(7):727–38.

68. Görisch SM, Richter K, Scheuermann MO, Herrmann H, Lichter P. Diffusion-limited compartmentalization of mammalian cell nuclei assessed by microinjected macromolecules. Exp Cell Res. 2003 Oct 1;289(2):282–94.

69. Frost TS, Jiang L, Lynch RM, Zohar Y. Permeability of Epithelial/Endothelial Barriers in Transwells and Microfluidic Bilayer Devices. Micromachines. 2019 Aug 13;10(8):533.

70. Wuhrer M, Stam JC, van de Geijn FE, Koeleman CAM, Verrips CT, Dolhain RJEM, et al. Glycosylation profiling of immunoglobulin G (IgG) subclasses from human serum. PROTEOMICS. 2007;7(22):4070–81.

71. Malek A. Role of IgG antibodies in association with placental function and immunologic diseases in human pregnancy. Expert Rev Clin Immunol. 2013 Mar 1;9(3):235–49.

72. Arroyo J, Torry RJ, Torry DS. Deferential regulation of placenta growth factor (PlGF)-mediated signal transduction in human primary term trophoblast and endothelial cells. Placenta. 2004 May;25(5):379–86.

73. Ricard N, Scott RP, Booth CJ, Velazquez H, Cilfone NA, Baylon JL, et al. Endothelial ERK1/2 signaling maintains integrity of the quiescent endothelium. J Exp Med. 2019 Jun 13;216(8):1874.

74. Chau K, Xu B, Hennessy A, Makris A. Effect of Placental Growth Factor on Trophoblast–Endothelial Cell Interactions In Vitro. Reprod Sci. 2020 Jun 1;27(6):1285–92.

75. Rahmouni K, Haynes WG. Endothelial effects of leptin: Implications in health and diseases. Curr Diab Rep. 2005 Jul 1;5(4):260–6.

76. Morrison MJ, Natale BV, Allen S, Peterson N, Natale DRC. Characterizing placental pericytes: Hypoxia and proangiogenic signalling. Placenta. 2024 Sep 26;155:1–10.

77. Harris SE, Matthews KSH, Palaiologou E, Tashev SA, Lofthouse EM, Pearson-Farr J, et al. Pericytes on placental capillaries in terminal villi preferentially cover endothelial junctions in regions furthest away from the trophoblast. Placenta. 2021 Jan 15;104:1–7.

78. Sharpe EE, Rosen MA, Rollins MD. 14 - Obstetric Analgesia and Anesthesia. In: Gleason CA, Sawyer T, editors. Avery's Diseases of the Newborn (Eleventh Edition) [Internet]. Philadelphia: Elsevier; 2024 [cited 2024 Oct 11]. p. 147-158.e3. Available from: https://www.sciencedirect.com/science/article/pii/B9780323828239000143

79. Utoguchi N, Chandorkar GA, Avery M, Audus KL. Functional expression of P-glycoprotein in primary cultures of human cytotrophoblasts and BeWo cells☆. Reprod Toxicol. 2000 May 1;14(3):217–24.

80. Castel G, Meistermann D, Bretin B, Firmin J, Blin J, Loubersac S, et al. Induction of Human Trophoblast Stem Cells from Somatic Cells and Pluripotent Stem Cells. Cell Rep. 2020 Nov 24;33(8):108419.

Lab on a Chip Accepted Manuscript

View Article Online
DOI: 10.1039/D5LC00075K

81. Zorzan I, Betto RM, Rossignoli G, Arboit M, Drusin A, Corridori C, et al. Chemical conversion of human conventional PSCs to TSCs following transient naive gene activation. EMBO Rep. 2023 Apr 5;24(4):e55235.

82. Karvas RM, Theunissen TW. Generation of 3D Trophoblast Organoids from Human Naïve Pluripotent Stem Cells. In: Zernicka-Goetz M, Turksen K, editors. Embryo Models In Vitro: Methods and Protocols [Internet]. New York, NY: Springer US; 2024 [cited 2024 Oct 2]. p. 85–103. Available from: https://doi.org/10.1007/7651_2023_496

83. Shannon MJ, McNeill GL, Koksal B, Baltayeva J, Wächter J, Castellana B, et al. Single-cell assessment of primary and stem cell-derived human trophoblast organoids as placenta-modeling platforms. Dev Cell. 2024 Mar 25;59(6):776-792.e11.

84. Sun C, James JL, Murthi P. Three-Dimensional In Vitro Human Placental Organoids from Mononuclear Villous Trophoblasts or Trophoblast Stem Cells to Understand Trophoblast Dysfunction in Fetal Growth Restriction. In: Raha S, editor. Trophoblasts: Methods and Protocols [Internet]. New York, NY: Springer US; 2024 [cited 2024 Oct 2]. p. 235–45. Available from: https://doi.org/10.1007/978-1-0716-3495-0_19

85. Hori T, Okae H, Shibata S, Kobayashi N, Kobayashi EH, Oike A, et al. Trophoblast stem cell-based organoid models of the human placental barrier. Nat Commun. 2024 Feb 8;15(1):962.

86. Carrion B, Janson IA, Kong YP, Putnam AJ. A Safe and Efficient Method to Retrieve Mesenchymal Stem Cells from Three-Dimensional Fibrin Gels. Tissue Eng Part C Methods. 2014 Mar;20(3):252–63.

Open Access Article. Published on 27 May 2025. Downloaded on 6/4/2025 8:36:13 AM.
This article is licensed under a Creative Commons Attribution 3.0 Unported Licence.

Lab on a Chip Accepted Manuscript

View Article Online
DOI: 10.1039/D5LC00075K

Title: Late-stage placental barrier model for transport studies of prescription drugs during pregnancy

Authors:

Sonya Kouthouridis[1] (kouthous@mcmaster.ca)
Poonam Saha[2] (poonam.saha@medportal.ca)
Madeleine Ludlow[3] (ludlowm@mcmaster.ca)
Boyang Zhang[1,3,*] (zhangb97@mcmaster.ca)

[1] Department of Chemical Engineering, McMaster University, Hamilton, ON, L8S 4L8, Canada
[2] Michael G. DeGroote School of Medicine, McMaster University, Hamilton, ON, L8S 4L8, Canada
[3] School of Biomedical Engineering, McMaster University, Hamilton, ON, L8S 4L8, Canada

*Correspondence to zhangb97@mcmaster.ca

Data Availability Statement
The datasets generated during the current study are available from the corresponding author upon reasonable request.

Open Access Article. Published on 27 May 2025. Downloaded on 6/4/2025 8:36:13 AM.
This article is licensed under a Creative Commons Attribution 3.0 Unported Licence.

Lab on a Chip Accepted Manuscript